UNIVERSIDADE DE LISBOA

FACULDADE DE CIÊNCIAS

DEPARTAMENTO DE BIOLOGIA VEGETAL

HEAVY METAL RESISTANCE IN EXTREMOPHILIC YEASTS:

A MOLECULAR AND PHYSIOLOGICAL APPROACH

Cátia Isabel Assis Fidalgo

MESTRADO EM MICROBIOLOGIA APLICADA

2011

UNIVERSIDADE DE LISBOA

FACULDADE DE CIÊNCIAS

DEPARTAMENTO DE BIOLOGIA VEGETAL

HEAVY METAL RESISTANCE IN EXTREMOPHILIC YEASTS:

A MOLECULAR AND PHYSIOLOGICAL APPROACH

Dissertação orientada por: Doutora Sandra Chaves e Prof.ª Doutora Ana Tenreiro

Cátia Isabel Assis Fidalgo

MESTRADO EM MICROBIOLOGIA APLICADA

2011

HEAVY METAL RESISTANCE IN EXTREMOPHILIC YEASTS:

A MOLECULAR AND PHYSIOLOGICAL APPROACH

Cátia Isabel Assis Fidalgo

2011

This thesis was fully performed at Center for Biodiversity, Functional and Integrative Genomics (BioFIG- FCUL) under the direct supervision of Dra. Sandra Chaves.

Prof.ª Dra. Ana Tenreiro was the internal designated supervisor and also participated as direct co-supervisor in the scope of the *Master in Applied Microbiology* of the Faculty of Sciences of the University of Lisbon.

Acknowledgments

First of all, I would like to acknowledge the fantastic support that my advisors, Sandra Chaves and Prof. Ana Tenreiro, gave me and, of course, all the advice and patience throughout the years.

Also, I would like to thank the research group leader, Prof. Rogério Tenreiro, for giving me the opportunity to carry out my thesis project in the Laboratory of Biotechnology and Microbiology in the Faculty of Sciences in the University of Lisbon, and for the support provided throughout my MsC.

Additionally, I would like to acknowledge Prof. Rui Malhó for all support provided in the fluorescence microscopy work and important input throughout this work. I would also like to thank Mário Gadanho for all the laboratory-related support and enlightenment regarding the background of this study.

I would especially like to acknowledge the very important support from my laboratory colleagues, the amazing BugWorkers, throughout the last years by supporting me and my work in the most diverse ways. Thank you!

Last, but not least, I would like to acknowledge the support from my friends, boyfriend, parents, brother, godmother and family in general: I could not have done this without you.

Abstract

Heavy metal resistant microorganisms are often associated with acidic environments, since metals are easily solubilized in acidic milieus. A unique yeast species from the *Cryptococcus* genus was isolated from two sulfur-rich acidic environments: acid mine drainage in the south of Portugal and a volcanic river in Argentina. The uniqueness of this species lies on the fact that it is the first acidophilic basidiomycetous yeast known to date. Additionally, the two strains chosen for this work (one from each environment) are resistant to high levels of heavy metals (arsenic, cadmium, copper and zinc). Metal resistance mechanisms are only described for neutrophilic yeasts, and mainly involve thiolated peptides and efflux transporters. To unveil the mechanisms that allow this *Cryptococcus* species to resist high levels of heavy metals, physiological, cytological and molecular approaches were conducted. Since both isolation sites are sulfur-rich, the possibility that this element influences metal resistance was assessed with microscale growth assays by determining minimal inhibitory concentrations of the four metals in differential sulfate availability conditions. Assessment of thiol-mediated resistance mechanisms was achieved by incubating cells (grown with and without metal) with the thiol-specific fluorescent probe 5-chloromethylfluorescein-diacetate. Dot blot hybridization was applied to detect gene homologues involved in arsenic extrusion, and vacuolar metal-thiol accumulation in response to arsenic and cadmium. Also, suppression subtractive hybridization was conducted to investigate resistance to cadmium by analyzing transcripts induced upon exposure to this metal. Our results indicate that thiolated peptides are involved in resistance to arsenic and zinc in the Portuguese strain, cadmium in the Argentinean strain, and copper in both strains. Also, both strains presented evidence of an arsenic extrusion mechanism, and of a Cd-induced demand in protein synthesis and folding. Thus, the present work allowed unveiling of heavy metal resistance mechanisms in two strains of this unique novel yeast species, *Cryptococcus* sp..

Keywords: Extremophilic yeasts, Heavy metal resistance mechanisms, Fluorescence microscopy, Differential gene expression, DNA hybridization.

Resumo

Existem diferentes critérios para definir 'metal pesado' que consideram diferentes características dos elementos metálicos. No entanto, o critério mais aceite consiste na comparação da gravidade específica do metal em relação à da água: metal pesado é aquele cuja gravidade específica é pelo menos cinco vezes superior à da água. Esta qualidade é atribuída a elementos essenciais como o cobre e o zinco, e a elementos não essenciais como o arsénio e o cádmio (Lide, 2009). Metais pesados, essenciais e não essenciais, podem ser tóxicos para todos os organismos, pelo que ao longo da evolução foram desenvolvidas diversas estratégias de destoxificação em resposta à presença destes elementos em excesso. Em microorganismos, este tipo de estratégias encontra-se principalmente caracterizado em organismos modelo com aplicações clínicas ou na indústria, como *Escherichia coli*, *Candida albicans*, *Saccharomyces cerevisiae* e *Schizosaccharomyces pombe*. No entanto, os níveis de resistência a metais pesados que estes microorganismos exibem é baixo em comparação com os níveis observados em microorganismos isolados de locais extremos, como por exemplo ambientes aquáticos ácidos ricos em metais pesados (Dopson *et al.*, 2003). Em leveduras, as principais estratégias descritas em leveduras consistem em mecanismos que levam à destoxificação do citoplasma (Perego & Howell, 1997; Tsai *et al.*, 2009). Estes podem ser exercidos por transporte dos metais para o exterior da célula, mediado por transportadores específicos, ou por acumulação dos metais, normalmente complexados com péptidos tiolados, em organitos como o vacúolo (revisto em Tamás & Wysocki, 2010).

Microorganismos resistentes a metais pesados estão frequentemente associados a ambientes acídicos, visto que a solubilização destes metais é facilitada em meios com pH baixo. Um exemplo deste tipo de ambiente existe na Faixa Piritosa Ibérica cuja extensão inclui o Rio Tinto, em Espanha, e as minas de São Domigos, no sul de Portugal. Dada a exploração de minérios associada a estes locais, os depósitos estáveis de minerais associados a diferentes metais foram expostos ao ar e água, o que conduziu à lenta reacção espontânea de oxidação desses mesmos minerais (Johnson & Hallberg, 2003). Comunidades de microorganismos litotróficos, presentes nas águas associadas a estes locais, aceleraram o processo de oxidação de minerais, visto que permitiram a regeneração de compostos necessários à reacção de oxidação. Um destes compostos, o ião férrico, em conjunto com o pH baixo permitiu uma manutenção da oxidação e lixiviação de metais que, dada a sua solubilidade mais facilitada em águas ácidas, ficam mais concentrados (López-Archilla *et al.*, 2001; Johnson & Hallberg, 2003). Este tipo de contaminação da água por oxidação de minerais expostos é denominado drenagem ácida de minas. A geologia local das minas de São Domingos é dominada por depósitos sulfúricos polimetálicos e inclui um lago particularmente extremo na Achada do Gamo, com o pH mais baixo de todos os lagos envolventes (pH 1.8) e com concentrações elevadas de enxofre e vários metais (Gadanho *et al.*, 2006). Por outro lado, ambientes aquáticos extremos com pH baixo e elevada concentração de metais podem ter uma origem relacionada com actividade vulcânica, como é o caso do Rio Agrio, localizado na Patagónia Argentina (Pedrozo *et al.*, 2001). Neste caso, a acidez da água do rio é uma consequência directa da produção de ácido sulfúrico no interior do vulcão, devido à actividade geotérmica e consequente emissão de gases do vulcão. Devido a interacções químicas, a acidez das águas leva a um desgaste da geologia vulcânica local e resulta em elevadas

concentrações de enxofre e metais na água (Pedrozo *et al.*, 2001; Russo *et al.*, 2008). Na parte superior deste rio (mais próxima do vulcão), o pH é de 2.2 e foram observadas concentrações elevadas de enxofre e metais pesados como ferro, zinco e arsénio (Russo *et al.*, 2008).

Uma nova espécie pertencente ao género *Cryptococcus* foi isolada em dois locais extremos distintos: Achada do Gamo, nas minas abandonadas de São Domingos (Gadanho *et al.*, 2006); e Rio Agrio, na Patagónia Argentina (Russo *et al.*, 2008). Para realizar o presente trabalho foram escolhidas duas estirpes desta espécie – uma de cada local. As estirpes desta espécie requerem pH baixo para crescer eficientemente, o que torna *Cryptococcus* sp. a primeira levedura basidiomicete acidófila conhecida até à data (Russo *et al.*, 2008). Adicionalmente, apresentam níveis de resistência a metais pesados mais elevadas que as toleradas por microorganismos modelo (Gadanho *et al.*, 2006).

No presente estudo foram pesquisados mecanismos pelos quais estas duas estirpes conseguem resistir a níveis elevados dos metais pesados arsénio, cádmio, cobre e zinco, tendo em consideração um eventual papel do enxofre nos mecanismos de resistência aos metais. Para tal, foram usadas abordagens experimentais a nível fisiológico, citológico e molecular.

As metodologias aplicadas incluíram ensaios de crescimento em microescala para determinar concentrações mínimas inibitórias para cada metal em diferentes condições de disponibilidade de sulfato. Por análise das diferenças nos níveis de resistência a cada metal pesado em condições diferenciais de sulfato, foi possível compreender a influência que a disponibilidade de sulfato exerce sobre os níveis de resistência a cada metal pesado. Foi também avaliado o eventual papel da forma química do composto metálico adicionado ao meio de cultura (arsenato *vs.* arsenito no caso do arsénio, e sulfato de metal *vs.* cloreto de metal para os outros metais).

A destoxificação de metais pesados por acumulação de péptidos tiolados está largamente descrita na literatura como sendo uma estratégia generalizada de resistência a metais pesados em leveduras. Por esta razão, a possibilidade da existência desta estratégia na espécie acidófila foi averiguada. Para tal, técnicas citológicas para observação em microscopia de fluorescência foram optimizadas e aplicadas nas duas estirpes, para os quatro metais pesados em estudo. As duas estirpes foram crescidas em meio com e sem metais pesados, e foram incubadas com uma sonda fluorescente específica para grupos tiolados, a diacetato-5-clorometilfluoresceína (CMFDA). A observação destas células em microscopia de fluorescência permitiu avaliar variações na intensidade de fluorescência provocadas pela presença dos metais. A observação de diferenças nas intensidades de fluorescência em condições diferenciais de crescimento (com metal *vs.* sem metal) foi interpretada como indicação de participação de péptidos tiolados nos mecanismos de destoxificação.

Foram também optimizadas e aplicadas metodologias de biologia molecular para averiguar a presença de homólogos de genes envolvidos no efluxo de arsénio, e de homólogos de um gene envolvido na acumulação de arsénio e cádmio no vacúolo da célula. A metodologia aplicada para este fim foi hibridação de DNA por 'dot blot' que consiste na utilização de uma sonda, que corresponde ao gene que se pretende detectar, com o DNA genómico das estirpes em análise. Os genes pesquisados incluíram dois homólogos de genes envolvidos no transporte de arsénio para o exterior da célula (*arsA* e *arsB*), e um homólogo de um gene envolvido na acumulação vacuolar de

arsénio e cádmio (*ycf1*). As sondas para esta hibridação foram obtidas por PCR a partir do DNA genómico da espécie-tipo do género *Cryptococcus*, *C. neoformans*. Para tal, foram desenhados primers 'forward' e 'reverse' para cada um dos três genes, e foram conduzidas reacções de PCR com um nucleótido marcado com digoxigenina (DIG-dUTPs). Os produtos de PCR obtidos foram então usados como sondas na procura de homologia dos genes indicados nas duas estirpes em estudo.

Neste trabalho foi também incluída uma abordagem transcriptómica para análise e identificação de genes diferencialmente expressos em células crescidas na presença e na ausência de cádmio. Para tal, foi extraído RNA de células obtidas em condições diferenciais (com e sem cádmio) em fase exponencial de crescimento e o mRNA foi purificado a partir do RNA total. Posteriormente, foi realizado um processo de hibridação subtractiva supressiva nas duas estirpes, no qual se obteve uma biblioteca de cDNA correspondente a transcritos cuja expressão foi aumentada na presença de cádmio. Após sequenciação, estes transcritos foram identificados comparação com bases de dados de sequências presentes no 'National Center for Biotechnology Information' (NCBI).

As metodologias aplicadas e consequente análise de resultados permitiram inferir sobre alguns aspectos das estratégias que as duas estirpes de *Cryptococcus* sp. analisadas utilizam na destoxificação de metais pesados. Nomeadamente, na estirpe Portuguesa predomina a evidência de que se trata de um mecanismo de resistência principalmente mediado por tióis, com possível subsequente acumulação no vacúolo da célula. Por outro lado, no caso da resistência ao arsénio na estirpe Argentina, o principal mecanismo de destoxificação parece ser mediado por efluxo do metal, possivelmente por um homólogo da bomba de efluxo ArsB, associada a uma ATPase homóloga de ArsA. Os resultados obtidos na resistência ao cádmio também indicam variabilidade intra-específica, uma vez que há indicação de um mecanismo de resistência mediado por tióis para a estirpe Argentina. No entanto, com base nos dados obtidos não foi possível sugerir um mecanismo específico para a estirpe Portuguesa. No caso da resistência ao cobre, os resultados sugerem a existência de um mecanismo mediado por tióis em ambas as estirpes, com a possibilidade de um mecanismo adicional que pode operar predominantemente na estirpe Portuguesa. Finalmente, a análise dos resultados obtidos sob exposição das leveduras a elevadas concentrações de zinco sugerem a possibilidade de acumulação deste metal em compartimentos celulares como o vacúolo.

Os resultados obtidos neste trabalho demonstram variabilidade intra-específica nos mecanismos de destoxificação de metais pesados em *Cryptococcus* sp., visto que nem sempre a mesma estratégia de resistência a metais pesados foi observada nas duas estirpes em estudo. Foi também verificada a possibilidade de existência de mais de um mecanismo de resistência a operar em simultâneo para apenas um metal, o que pode justificar a elevada resistência a metais pesados observada nas duas estirpes estudadas. Os mecanismos de destoxificação nesta levedura única deverão, então, ser alvo de análise em maior detalhe em investigação futura.

Palavras-chave: Leveduras extremófilas, Mecanismos de resistência a metais pesados, Microscopia de fluorescência, Expressão diferencial de genes, Hibridação de DNA.

Index

1. Introduction

1.1. Metals and metal resistance

Classification of metallic elements

Metallic elements can be classified considering a number of characteristics. In a biological perspective, metals are either considered essential or nonessential, taking into account their biological function. Essential metals exert functions on biological reactions or are part of the composition of biological components, such as metalloproteins (Waldron *et al*., 2009). These metals usually have their cytosolic levels tightly regulated through homeostasis mechanisms and are typically maintained within a narrow range. On the other hand, nonessential metals are not necessary for cell function, are usually toxic in very low concentrations and lack homeostasis mechanisms. Nevertheless, excessive concentrations of both essential and nonessential metals can be cytotoxic and even cause cell death (Hall, 2002).

A different metal classification considers chemical reactivity and relies on the affinity to bind certain ligands. Metals that present high affinity to react with sulfhydryl (thiol) groups are considered *soft* metals, in contrast with *hard* metals, which preferably bind oxygen. A third alternative is considered when metals are able to bind sulfur, oxygen or nitrogen atoms (Summers, 2009). In general, the abovementioned group of nonessential metals falls under the soft metal category and is highly related to cell toxicity, since the reaction with thiol groups may lead to functional impairment of many proteins. This chemical property is, nonetheless, explored by cells for metal detoxification (reviewed in Tamás & Wysocki, 2010).

Some metals are considered heavy metals and the difference between heavy and non-heavy metals has been subject of discussion (Duffus, 2002). The most used parameter for this classification consists in the ratio of specific gravity of the metal *vs.* the specific gravity of water at 1 to 4ºC. Considering this parameter, several thresholds have been used to define what is considered *heavy*, but none is globally accepted (Duffus, 2002). The most accepted and applied threshold is a specific gravity ratio >5 to define a heavy metal (Lide, 2009).

Finally, some elements in the periodic table are considered metalloids (or semi-metals), since they present intermediary physiochemical properties between those of metals and nonmetals (Tamás *et al.*, 2006).

In the present work, the four heavy metal(loid)s under study (one heavy metalloid and three heavy metals) are considered *heavy* by the most accepted definition (specific gravity ratio >5) and comprise essential and nonessential elements. Metal(loid) toxic effects and detoxification responses in yeasts will be analyzed in more detail in the following sections.

Metal(loid)-induced cellular damage and toxicity

Although some metals are necessary as micronutrients for biological activities, all elements are toxic when present in excess. As a consequence, living organisms have evolved different strategies of metal(loid) detoxification during evolution to cope with metal(loid)-induced toxicity. Metal(loid) toxicity can be viewed as a consequence of oxidation state, speciation, complex form, concentration and interaction with cellular components (Summers, 2009). Metal(loid) availability is highly important for toxicity, since it determines uptake, intracellular distribution and interaction with molecules. In general, metal(loid) exposure can lead to oxidative stress, impairment of DNA repair systems, alteration of protein function and interference with membrane fluidity (reviewed in Beyersmann & Hartwig, 2008).

In the present work, the following heavy metal(loid)s were studied: Arsenic (As; metalloid), Cadmium (Cd), Copper (Cu) and Zinc (Zn). Some specific toxic effects and cellular targets of these heavy metal(loid)s are listed in Table 1.

Table 1 Toxic effects and cellular targets of the metal(loid)s Arsenic (As), Cadmium (Cd), Copper (Cu) and Zinc (Zn). Information in Beyersmann & Hartwig (2008), Thorsen *et al*., (2009) and Tamás & Wysocki (2010).

Heavy metal(loid)	Toxic effects at the cellular level
As	Indirect oxidative stress: • Indirect Fenton-type reactions • Protein oxidation and lipid peroxidation Inhibition of tubulin and actin polymerization Interference with DNA: • Decreased DNA repair • Genomic instability
Cd	Indirect oxidative stress: • Indirect Fenton-type reactions, leading to lipid peroxidation • Inhibition of antioxidant enzymes Replacement of calcium and Zn ions in proteins Iron depletion Interference with DNA: • DNA mismatch repair system • DNA replication
Cu	Oxidative stress: • Direct Fenton-type reactions • Protein oxidation and lipid peroxidation • DNA damage Iron depletion
Zn	Indirect oxidative stress: • Indirect Fenton-type reactions Iron depletion

Oxidative stress is caused by reactive oxygen species (ROS) formed in the presence of agents such as metal(loid)s. When ROS reach toxic levels, nearly all cellular components can be damaged. Ultimately, oxidative stress may result in lipid peroxidation, protein oxidation and DNA damage. Some metal(loid)s are considered redox active, as they undergo redox-cycling reactions, while others are

considered redox inactive. The latter can, however, lead to oxidative stress by indirect mechanisms, such as enzyme inactivation and antioxidant pool depletion (reviewed in Beyersmann & Hartwig, 2008).

More specifically, As ions are redox active and are able to lead to redox reactions in biological systems by indirect Fenton-type reactions, resulting in ROS accumulation in the cell. This indirect ROS production induced by As leads to more toxic effects than the direct binding of the metalloid to proteins (Samikkannu *et al*., 2003). Ultimately, oxidative stress induced by As results in lipid peroxidation and protein oxidation (reviewed in Tamás & Wysocki, 2010). In addition, the oxidation state of this metalloid influences its toxicity, as the pentavalent form arsenate (As(V)) is less toxic than the trivalent form arsenite (As(III); Oremland & Stolz, 2003). As(V) is a molecular analog of phosphate and becomes cytotoxic by inhibiting oxidative phosphorylation. As(III), on the other hand, is more toxic due to its ability to bind to thiol groups and consequently impair the function of many proteins (Haugen *et al*., 2004; reviewed in Tamás *et al.*, 2006).

Cu is also a redox active metal and frequently leads to the formation of hydroxyl radicals by Fenton-type reactions. Cu-related oxidative stress results in lipid peroxidation, oxidative protein damage and DNA damage (reviewed in Beyersmann & Hartwig, 2008).

On the other hand, Cd and Zn are redox inactive and, consequently, do not directly participate in redox reactions. The toxic effects of Zn excess, apart from indirect participation in Fenton reactions, are not well known in yeasts. The nonessential metal Cd is able to cause oxidative stress indirectly, by inhibiting the activity of antioxidant enzymes (reviewed in Beyersmann & Hartwig, 2008, and in Tamás & Wysocki, 2010).

Some metal ions present similar physiochemical properties as those of essential ions (e.g. charge and radius size). These properties allow the toxic metal ions to replace essential ions in cellular components, possibly resulting in functional impairment of those components (reviewed in Beyersmann & Hartwig, 2008). Cd ions easily replace calcium (Ca) ions in biological systems, since both present the same charge and have similar radius. Despite the higher affinity of Cd to bind sulfur, and Ca to bind oxygen, Cd is able to bind to oxygen and replace Ca in proteins, leading to toxic effects. Cd can also replace Zn in proteins, despite the difference in radius size. In this case, protein function is usually disturbed or abolished, and the most affected proteins are transcription factors. Cd may substitute Zn ions in Zn-finger domains of DNA repair proteins, disturbing their correct function within the DNA repair complex and potentially leading to the inactivation of DNA repair systems (reviewed in Beyersmann & Hartwig, 2008). In addition to sensibility to Cd ions, Zn-fingers are potential targets for other toxic metal(loid)s. In Zn-finger domains, Zn is complexed through four invariant cysteine (Cys) and/or histidine residues, allowing not only DNA-binding but also protein-protein interactions. The thiol side chain present in Cys residues is susceptible to oxidation by many toxic compounds, such as As(III). In this case, As(III) reacts with thiol groups in Zn-finger domains, leading to diminished DNA repair or altered DNA methylation patterns (reviewed in Beyersmann & Hartwig, 2008).

Overall, it is clear that metal(loid)s lead to toxicity through a number of mechanisms and cellular targets. Some of these mechanisms and targets are common to different metallic elements, while others are metal(loid)-specific.

Metal(loid) uptake and detoxification systems

Microbes have evolved mechanisms in order to cope with the presence of metal(loid)s. These mechanisms can either be directed towards homeostasis for essential metals, or detoxification for nonessential and excess essential metal(loid)s. Studies regarding metal(loid) detoxification mechanisms in microbes have been conducted in prokaryotes and eukaryotes. In neutrophilic and, more recently, acidophilic prokaryotes, detoxification mechanisms have been identified and characterized. Most available information refers to neutrophilic prokaryotes, despite the fact that microbes surviving in acidic metal(loid)-rich environments should possess the most advanced detoxification mechanisms, making them ideal systems to study and improve understanding of metal(loid) resistance (Dopson *et al.*, 2003).

Information available for metal(loid) detoxification mechanisms in yeasts only considers neutrophilic yeasts and there is considerably less information available when compared to prokaryotes. In addition, the studied neutrophilic yeasts are mainly model organisms, belonging to the ascomycetous group, such as *Saccharomyces cerevisiae*, *Schizosaccharomyces pombe* and *Candida albicans*. Literature in model yeasts indicates that upon metal(loid) exposure the main goal of the yeast cell is to detoxify the cytoplasm by rendering the metal ions unavailable to promote cytotoxic effects. This cytoplasmic detoxification can be achieved by metal(loid) transport to the outside of the cell, or to lesser sensitive cellular compartments, such as the vacuole (reviewed in Tamás & Wysocki, 2010). An alternative mechanism can be observed in these model yeasts where the metallic compounds do not reach the cytoplasm: biosorption. This mechanism includes bioaccumulation and the precipitation/chelation of the metal at the cell wall, and is highly dependent on cell wall characteristics. The structure and the distribution of homopolysaccharides (mannans and glucans), single saccharides and acid components, which are good binding agents, dictate the cell wall's biosorption capacity (reviewed in Raspor & Zupan, 2006). Nevertheless, the main metal(loid) detoxification mechanisms in yeast remain those that allow cytoplasmic detoxification (reviewed in Tamás & Wysocki, 2010), and are described in greater detail in the following paragraphs.

In general, essential metals enter yeast cells by dedicated transporters, which are often a target of negative regulation when the specific metal is present in excess intracellularly. On the other hand, nonessential metal(loid)s do not enter yeast cells via dedicated transporters. Instead, these metals are able to use some transporters for essential ions (reviewed in Tamás & Wysocki, 2010). More specifically, As uptake can be mediated in the As(V) or As(III) chemical form, through different transporters: As(V) enters cells through phosphate transporters (Figure 1A); while As(III) enters the cell by aquaglyceroporins (Fps1) or hexose permeases. The chemical form $As(OH)_3$ is similar to

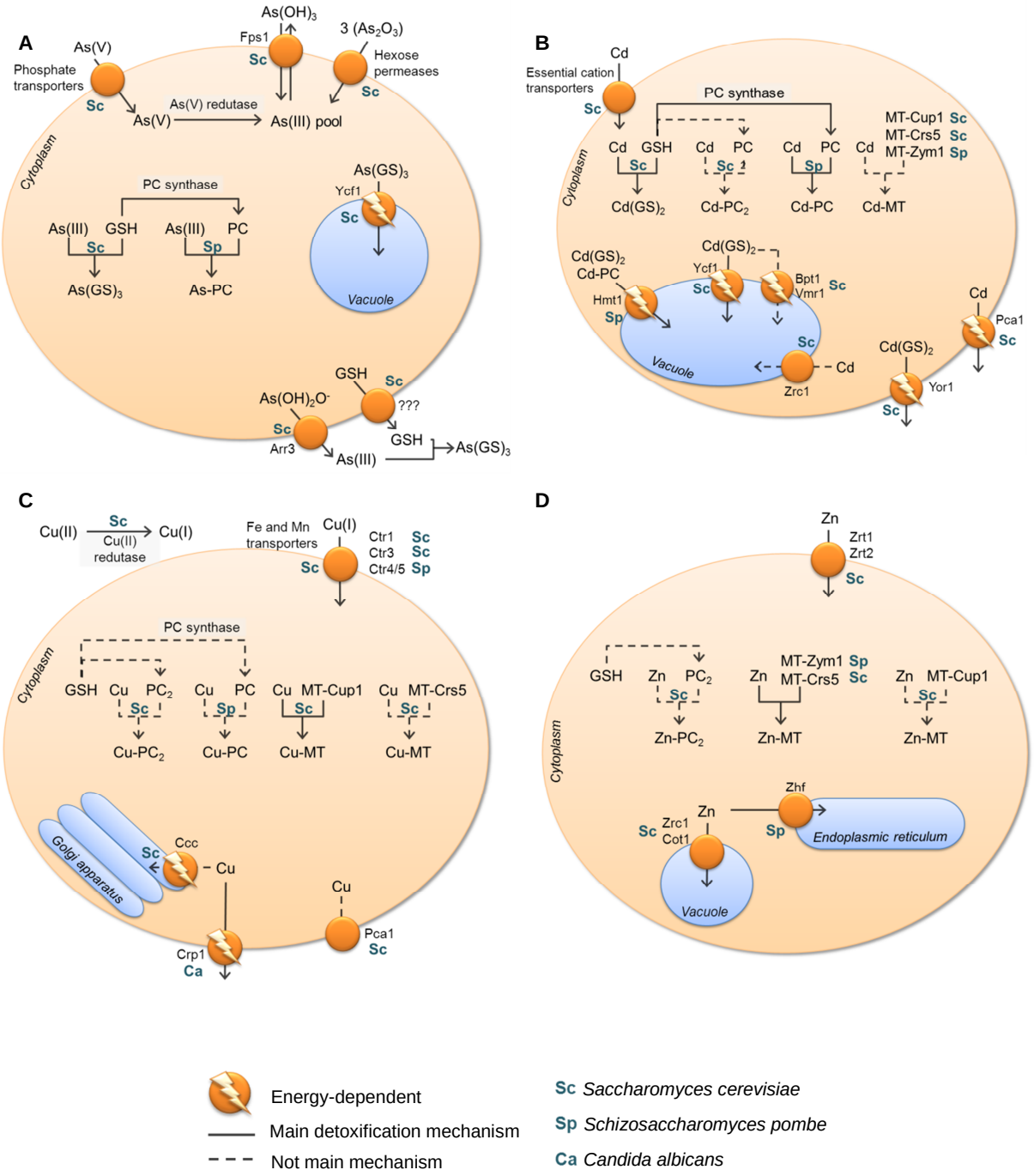

Figure 1 Schematic representation of heavy metal(loid) uptake and detoxification pathways known to operate in yeasts. Nonessential metal(loid)s As (**A**) and Cd (**B**) enter the cell through transporters for essential ions, while essential heavy metals Cu (**C**) and Zn (**D**) enter the yeast cell through dedicated transporters. Detoxification of excess metal(loid)s in yeast mainly occurs through cytoplasmic detoxification, which can be achieved by metal(loid) efflux and/or metal(loid) transport to lesser sensitive cellular compartments, such as the vacuole. Cytoplasmic detoxification based on chelation with thiolated peptides – such as glutathione (GSH), phytochelatins (PC_2 and PC) and metallothioneins (MT) – is widely observed in yeast. See text for detail. Based on information from Carri *et al.* (1991), Kneer *et al.* (1992), Dancis *et al.* (1994), Li *et al.* (1997), Perego & Howell (1997), Yuan *et al.* (1997), Clemens *et al.* (1999), Mukhopadhyay *et al.* (2000), Peña *et al.* (2000), Weissman *et al.* (2000), Tamás & Wysocki (2001), Borrelly *et al.* (2002), Rosen (2002), Sharma *et al.* (2002), Nagy *et al*. (2006), Tamás *et al.* (2006), Adle *et al.* (2007), Pagani *et al*. (2007a), Prévéral *et al.* (2006), Simm *et al.* (2007), Prévéral *et al.* (2009), Tsai *et al.* (2009), Maciaszczyk-Dziubinska *et al.* (2010a and 2010b), Tamás & Wysocki (2010) and Beaudoin *et al.* (2011).

glycerol, allowing uptake through the aquaglyceroporin. On the other hand, in the As_2O_3 form, a structure similar to a hexose is formed upon polymerization of three As_2O_3 molecules. Cd uptake systems mostly comprise transporters involved in the uptake of essential cations (Figure 1B), such as Zn, Ca, Manganese and Iron (reviewed in Tamás & Wysocki, 2010).

Essential metal uptake, as mentioned above, occurs through dedicated transporters. For Cu, these transporters belong to the Ctr gene family (Figure 1C): in the baker's yeast, *S. cerevisiae*, Ctr1 (Dancis *et al.*, 1994) and Ctr3 (Peña *et al.*, 2000) are responsible for the uptake of the essential cation as Cu(I). Prior to uptake, divalent copper is reduced outside the cell by a Cu(II) reductase in *S. cerevisiae*. In the fission yeast *S. pombe*, Cu is transported by a Ctr4/5 complex (Beaudoin *et al.*, 2011). For Zn, two dedicated transporters are described in yeasts (Figure 1D): the high affinity transporter Zrt1 and the low affinity transporter Zrt2 (reviewed in Tamás & Wysocki, 2010).

Once inside the yeast cell, metal(loid)s often react with thiol groups present in Cys residues, and these reactions may impair protein function, as described before. However, thiolated peptides can be produced to chelate metal(loid)s, reducing their reactivity and availability to exert toxic effects. Such thiolated peptides include the enzymatically synthesized glutathione (GSH) and phytochelatins (PC), and the gene-coded low molecular weight metallothioneins (MT; reviewed in Tamás & Wysocki, 2010). The resulting metal-thiolated peptide complexes may be used as a substrate for metal(loid) extrusion to the outside of the cell, or for accumulation in cellular compartments such as the vacuole (Figure 1).

GSH is a tripeptide (L-γ-Glu-Cys-Gly), enzymatically synthesized by two enzymes in the cytoplasm in an energy-dependent manner (Suzuki *et al.*, 2011). This peptide the main antioxidant agent inside yeast cells and plays a great role in protecting the cell against oxidative stress, which is one of the main toxic effects exerted by metal(loid)s in yeast cells (Table 1). GSH detoxifies ROS, is involved in the modulation of gene expression, in redox signaling, and in the regulation of enzymatic activities (Zechmann *et al.*, 2011). Additionally, the thiol group present in the Cys residue of GSH reacts with As(III), Cd, and Cu with lower affinity, to form a GS-metal(loid) complex (Figure 1A-C; reviewed in Tamás & Wysocki, 2010).

In *S. pombe*, the small metal(loid)-binding peptides PC ($(\gamma\text{-Glu-Cys})_n$Gly) are synthesized by the constitutively expressed PC synthase (PCS) in the presence of some metal(loid)s. PCS uses GSH as a substrate, yielding the enzymatically synthesized Cys-rich small peptides (Clemens *et al.*, 1999). Due to the thiol groups present in Cys residues, PCs are able to bind metal(loid)s, in the same fashion as GSH. This is mainly the case in detoxification of As(III), Cd (Figure 1A-C; Prévéral *et al*., 2006; reviewed in Tamás & Wysocki, 2010).

In *S. cerevisiae*, PC synthesis has also been described. In this case, however, PCS is not involved and only two GSH molecules are used, yielding PC_2 (Kneer *et al.*, 1992). These PC_2 molecules were associated with Cd, Cu and Zn detoxification, but were not considered main pathways for detoxification of these heavy metals (Figure 1B-D; reviewed in Tamás & Wysocki, 2010).

Finally, MTs are gene-coded low molecular weight Cys-rich proteins that protect yeast cells against a broad range of metals (reviewed in Tsai *et al.*, 2009). The most described yeast MT is the Cup1 of *S. cerevisiae*, which is mainly associated with Cu detoxification (reviewed in Tamás & Wysocki, 2001). Carri *et al.* (1991) described Cup1 as not being involved in Cd detoxification. However, several authors attributed Cd, in addition to Cu, detoxification to chelation by this MT (Perego & Howell, 1997; reviewed in Tamás & Wysocki, 2001).

Furthermore, the MTs Crs5 (*S. cerevisiae*; Pagani *et al.*, 2007a) and Zym1 (*S. pombe*; Borrelly *et al.*, 2002) are described as the main MTs associated with Zn detoxification. These MTs have also been associated to Cd detoxification in yeasts, although not as a main detoxification mechanism (Figure 1B; reviewed in Tamás & Wysocki, 2010).

Metalloid detoxification, in the case of As(V), involves reduction to As(III) by an As(V) reductase in the cytoplasm (Figure 1A; Mukhopadhyay *et al*., 2000). Three families of arsenate reductases have been described and all involve binding of As(V) to thiol groups in Cys residues followed by participation of a sulfate intermediate to yield As(III) (reviewed in Rosen, 2002). Consequently, despite the As chemical form that enters the cell, an As(III) pool can be viewed as the target for As detoxification. In *S. cerevisiae*, a predominant As(III) detoxification mechanism consists in transport of $As(GS)_3$ complexes to the vacuole through the transporter Ycf1 (Prévéral *et al.*, 2006). Alternatively, As(III) may be extruded from the cell by the aquaglyceroporin Fps1, in a concentration gradient manner (Maciaszczyk-Dziubinska *et al.*, 2010a), or by the As(III)-specific transporter Arr3 (also known as Acr3; Maciaszczyk-Dziubinska *et al.*, 2010b). The latter transporter facilitates the efflux of the $As(OH)_2O^-$ anion, coupled to the membrane potential (reviewed in Tamás & Wysocki, 2010). Recently, an additional mechanism has been proposed for *S. cerevisiae*. In this mechanism, GSH is extruded to the outside of the cell, by an unknown transporter, and $As(GS)_3$ complexes are formed, as As(III) exits the cell through Arr3. As a result, these $As(GS)_3$ complexes cannot re-enter the cell by the Fps1 transporter. Additionally, this extracellular metalloid chelation would alter the concentration gradient of $As(OH)_3$, the substrate of Fps1. As a consequence, this aquaglyceroporin would be able to extrude $As(OH)_3$ form the cell (unpublished data reviewed in Tamás & Wysocki, 2010).

In *S. pombe*, the presence of the metalloid in the cytoplasm binds to the constitutively expressed PCS and lowers its turnover rate. As a consequence, PC is synthesized and As(III)-PC complexes are formed, resulting in the main form of As(III) detoxification in the fission yeast (reviewed in Tamás & Wysocki, 2010).

Cd detoxification mechanisms in yeasts are highly associated with thiolated peptides (Figure 1B). In fact, $Cd(GS)_2$ complexes have been described as a substrate for transport to the outside of the cell, by the Yor1 transporter in *S. cerevisiae* (Nagy *et al.*, 2006) and to the vacuole, by different transporters. In this yeast, the vacuolar transport of $Cd(GS)_2$ by Ycf1 has also been described (Li *et al.*, 1997), operating in a similar way to $As(GS)_3$ detoxification (see above). To a lesser extent, the

same substrate is transported by Bpt1 in the baker's yeast (Sharma *et al.*, 2002; reviewed in Tamás & Wysocki, 2010). In the fission yeast *S. pombe*, however, vacuolar accumulation of Cd-thiolated peptides complexes occurs through Hmt1. This transporter has been associated with vacuolar accumulation of $Cd(GS)_2$ complexes (reviewed in Tsai *et al.*, 2009) and was recently shown to be a polyvalent transporter, in the sense that Hmt1 can also transport Cd-PC complexes (Prévéral *et al*., 2009).

An additional Cd detoxification mechanism by efflux has been identified in *S. cerevisiae*, where thiols are not implicated. In this case, Cd extrusion is accomplished by the plasma membrane transporter Pca1, a Cd efflux pump. In the presence of this toxic metal, the turnover rate of Pca1 is decreased and the transporter is directed to the plasma membrane (Adle *et al.*, 2007). Interestingly, Pca1 is usually nonfunctional in common laboratory strains of the baker's yeast, since these strains generally harbor a missense mutation in a conserved residue that results in loss of function (Adle *et al.*, 2007; reviewed in Tamás & Wysocki, 2010).

As denoted above, thiolated peptides in general play a significant role in Cd detoxification mechanisms in yeasts. In fact, the presence of this heavy metal in *S. cerevisiae* cells was described as being responsible for a phenomenon called *sulfur sparing* (Figure 2; Fauchon *et al.*, 2002). Upon exposure to Cd, the yeast cells respond by converting most of the intracellular sulfate pool into GSH, thus causing a decline in the sulfate available for protein synthesis. Cells adapt to this vital metabolite requirement by reducing the production of abundant sulfur-rich proteins, as protein synthesis becomes highly conditioned by the necessity to produce considerable amounts of GSH (Fauchon *et al.*, 2002).

In sulfur sparing, some abundant glycolytic enzymes are replaced by sulfur-depleted isozymes. The difference in amino acid occurrence is specific to methionine and Cys and is more pronounced for Cys residues, as the synthesized sulfur amino acids are mostly used for GSH biosynthesis. This adaptation works mainly on the most abundant proteins, regardless of their function, as expected for a significant sulfur saving (Fauchon *et al.*, 2002; and reviewed in Tamás & Wysocki, 2010).

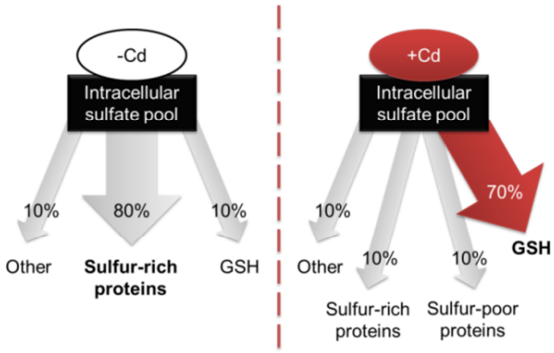

Figure 2 Schematic representation of Cd-induced sulfur sparing. In the left panel, in normal cell metabolism in yeast, the greater portion of the intracellular sulfate pool is used in the synthesis of sulfur-rich proteins. Upon exposure to elevated concentrations of Cd (right panel) the intracellular sulfate pool suffers a deviation from the synthesis of sulfur-rich proteins to the synthesis of GSH. Additionally, some abundant sulfur-rich enzymes are replaced by sulfur-poor isozymes. Based on information available in Fauchon e*t al.* (2002); representation adapted from Tamás *et al.* (2006).

Cu detoxification in *S. cerevisiae* is highly associated with the Cu-induced MT Cup1 (Figure 1C). This MT protects the yeast cell from oxidative stress and toxic levels of metallic ions (reviewed in Tamás & Wysocki, 2010). An additional intracellular detoxification mechanism for Cu relies on the activity of the P-type ATPase Ccc2 in *S. cerevisiae* and in *S. pombe* (Weissman *et al.*, 2000). However, Cu transport by Ccc2 is described as restricted to the Golgi compartment, as part of the secretory pathway, not being considered to play a significant role in Cu detoxification (Yuan *et al.*, 1997).

Cu detoxification may also be achieved by the Cd transporter Pca1. However, the detoxification mechanism for this metal does not depend on metal translocation, which was the case for Cd. A Cys-rich region located in the N-terminus of Pca1 sequesters Cu and detoxification is achieved in this sense (Adle *et al*., 2007). Nevertheless, Cu detoxification may be accomplished in yeasts by metal translocation through the plasma membrane. This is accomplished by Crp1, identified in *C. albicans*, which resists higher Cu levels than the *S. cerevisiae* (Weissman *et al.*, 2000).

As denoted by Pagani *et al*. (2007a), in contrast with the large amount of knowledge gathered on the response to zinc depletion, little is known about the molecular responses triggered by zinc overload beyond the participation of the vacuolar-sequestering pathway. In *S. cerevisiae*, Zn detoxification requires two vacuolar transporters, Zrc1 and Cot1 (Figure 1D; Simm *et al*., 2007). These authors observed a capacity for vacuolar accumulation of 100 mM of this cation, which is considered to be close to the maximum Zn tolerated concentration for the baker's yeast. On the other hand, the fission yeast *S. pombe* accumulates surplus Zn intracellularly, in the endoplasmic reticulum, through the Zhf1 transporter (Borrelly *et al.*, 2002).

An alternative intracellular Zn detoxification mechanism was identified in yeast and is mediated by Zn-induced MTs: Crs5 in *S. cerevisiae* (Pagani *et al.*, 2007a) and Zym1 in *S. pombe* (Borrelly *et al.*, 2002).

1.2. Extreme acidic environments

Acidic water bodies are a type of extreme environment characterized by low pH and often associated with elevated metal(loid) concentrations, since low pH promotes the solubilization of metallic compounds. These extreme environments may have a natural or an anthropogenic origin and the latter is frequently related to mining activities (Johnson & Hallberg, 2003).

The Iberian Pyrite Belt (IPB) is a vast mining area that comprises the south of Spain and Portugal. The IPB is one of the most important pyrite (FeS_2) regions in the world due to its complex polymetallic sulfide deposits. In the south of Portugal, the IPB includes the São Domingos' mines (SDM). These abandoned copper-iron mines represent an example of acid mine drainage (AMD), a well-known type of extreme acidic environment.

AMD is a consequence of the oxidative solubilization of exposed minerals, especially sulfides, in the presence of ferric iron (Fe^{3+}). This compound acts as an oxidant and is of major importance in mineral oxidation in AMD generation. Some minerals, such as FeS_2, are stable when both water and oxygen are excluded. However, the unearthing of geological formations, as a result of mining activities, exposes the minerals to water and oxygen (Figure 3A). Very slowly, spontaneous abiotic reactions oxidize minerals, using Fe^{3+} as an oxidant, yielding reduced inorganic sulfur compounds (RISCs; e.g. $S_2O_3^{2-}$). Proton acidity increases as a by-product of the previous reaction and facilitates the solubilization of metallic compounds. The resulting conditions allow the establishment of acid-tolerant and/or acidophilic prokaryotes that are able to thrive in metal(loid)-rich waters.

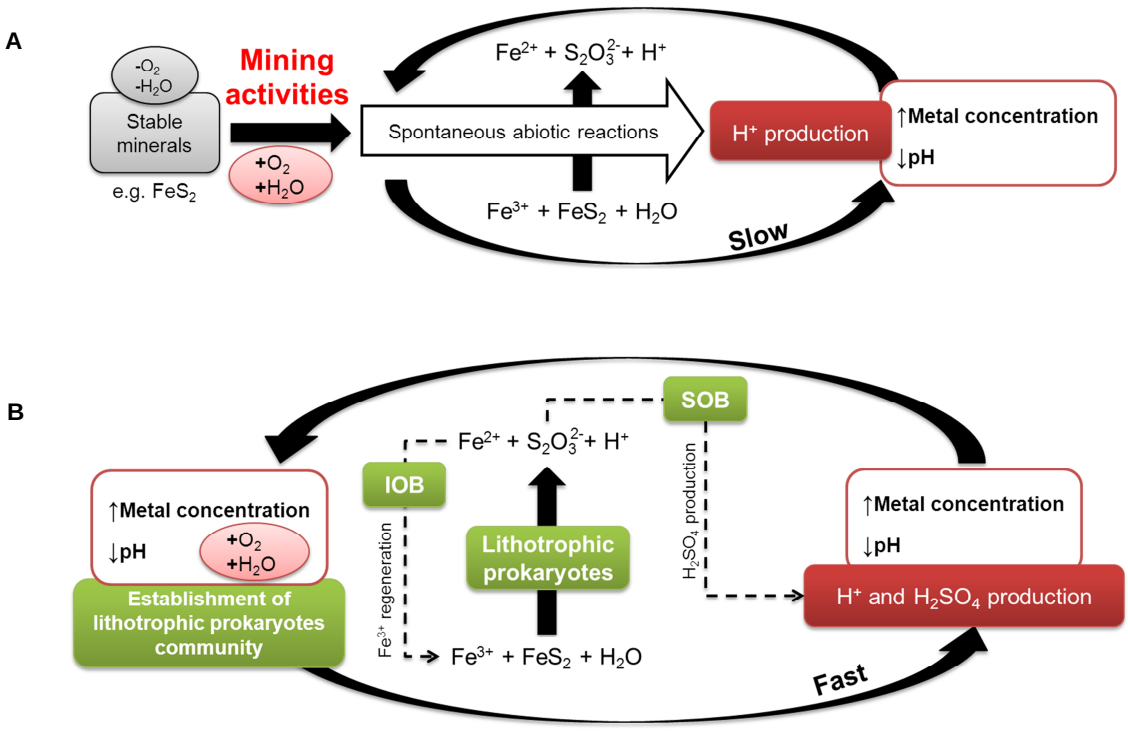

Figure 3 Schematic representation of the establishment and maintenance of acidic pH and high metal concentration in AMD waters. **A** Initial and slow establishment of an extreme environment, as a consequence of mining activities and spontaneous abiotic reactions. First, the presence of ferric iron (Fe^{3+}) allows mineral oxidation, acting as an oxidant. As a result, reduced inorganic sulfur compounds (RISCs, e.g. $S_2O_3^{2-}$) are formed and proton acidity increases as a by-product of the mineral oxidation reaction. Slowly, an acidic environment is established which facilitates the solubilization of metallic compounds. **B** The previously settled extreme environment allows the establishment of a microbial community of lithotrophic prokaryotes. Iron oxidizing bacteria (IOB) present in this community regenerate Fe^{3+}, allowing faster mineral oxidation reactions. Sulfur oxidizing bacteria (SOB) use RISCs as a substrate for sulfuric acid production, further contributing to an acidic environment. Based on information in López-Archilla *et al*. (2001), and reviewed in Johnson & Hallberg (2003).

Upon establishment of this community of lithotrophic prokaryotes, the mentioned reaction of RISCs oxidation is highly accelerated (Figure 3B). This enhanced efficiency of mineral oxidation reactions is especially due to the fact that iron oxidizing bacteria (IOB; López-Archilla *et al*., 2001) in the community are able to perform cycles of Fe^{3+} regeneration, which is required for further mineral oxidation. Additionally, sulfur oxidizing bacteria (SOB) present in the microbial community are able to produce sulfuric acid, using RISCs as a substrate. In summary, the presence of this microbial community allows the establishment of a much more extreme environment and the maintenance of the extreme conditions (reviewed in Johnson & Hallberg, 2003).

Naturally acidic environments can be found in water bodies near volcanic activity. An example of this type of extreme environment is the Lake Caviahue in the Argentinean Patagonia. The nearby Copahue volcano releases metals as naturally existing minerals through volcanic activity (Pedrozo *et al.*, 2001). This natural process of volcanic geothermal activity and consequent gas expulsions are responsible for the acidity verified in Lake Caviahue, since sulfuric acid is originated in the headwaters of the river in the volcano. In a parallel to the AMD situation, the acidic waters weather the local volcanic geology and lead to elevated concentrations of different metal(loid)s. The microbial community present in this naturally acidic environment also allows the enhancement and maintenance of the extreme characteristics (Pedrozo *et al.*, 2001; Russo *et al.*, 2008).

Succinctly, extreme acidic environments with different origins can lead to the same results: low pH and elevated concentrations of metal(loid)s. In the first given example, the Portuguese AMD site, there is one particularly acidic pond, named Achada do Gamo, which presents pH=1.8 (Gadanho & Sampaio, 2006). In the example of a natural acidic environment, a main inflow of Lake Caviahue, the Upper region of the River Agrio (URA) presents a similar acidity value, with pH=2.2 (Russo *et al.*, 2008). Both sites present elevated concentrations of sulfur and different metal(loid)s, as described in Table 2.

Table 2 Metal and sulfur concentrations (mM) from two extreme sites: acid mine drainage in Achada do Gamo, Portugal (PRT; Gadanho & Sampaio, 2006, and Gadanho, personal communication) and upper River Agrio in Argentina (ARG; Russo *et al.*, 2008).

	Arsenic	**Cadmium**	**Copper**	**Zinc**	**Iron**	**Sulfur**[¥]
PRT	0.64	0.04	10.07	0.006	160.98	306.25
ARG	12.29[†]	n. d.	b. d. l.	0.12	1.24	74.85

n. d. – not described. b. d. l. – below detection level.

[†]Information available in Pedrozo *et al.*, 2001.

[¥]Sulfur was measured as total sulfur in the PRT site and as sulfate in the ARG site.

Considering the extreme nature of the described AMD and volcanic sites, the organisms that are able to live in these conditions must have evolved metal resistance mechanisms. Interestingly, despite the highly important role that the prokaryote community plays in the maintenance of the above described extreme environments, studies conducted in acidic waters of the IPB revealed that eukaryote microbes, such as yeasts, are the main biomass contributors (Zettler *et al.*, 2002; Gadanho & Sampaio, 2006).

Taking into account the impact that elevated metal concentrations may have on the environment and public health, the study of metal resistance mechanisms is of great importance.

1.3. An extremophilic yeast: *Cryptococcus* sp.

An undescribed species of the *Cryptococcus* genus has been isolated from the two extreme environments described above: Achada do Gamo in SDM in Portugal (Gadanho *et al.*, 2006) and URA in Argentinean Patagonia (Russo *et al.*, 2008).

Gross & Robins (2000) suggested that fungi living in acidic habitats should be regarded as acid-tolerant rather than acidophilic, since they are also able to grow under neutral or even alkaline pH conditions. However, isolates from this *Cryptococcus* species require low pH for optimal growth (Gadanho *et al.*, 2006; Russo *et al.*, 2008), a physiological requirement that has only been observed in a species of *Candida*, *C. sorbophila*, which presents an optimum growth ah pH 2.5-3 (De Silóniz *et al.*, 2002). Consequently, these species should be considered acidophilic, and the yeast species under study in the present work represents the only acidophilic basidiomycetous yeast discovered to date.

The ascomycetous yeast *C. sorbophila* was found to resist Zn to higher levels than the model yeast *S. cerevisiae* (De Silóniz *et al.*, 2002). However, strains from the *Cryptococcus* species under study resist high concentrations of several metals, higher than those presented by model organisms (Gadanho *et al.*, 2006).

In the present work, two strains of *Cryptococcus* sp., one from each isolation effort described above, were chosen for the study of heavy metal resistance mechanisms: MSD44 (from Achada do Gamo) and CRUB1564 (from URA). These strains were chosen as a result of their pH requirements, high metal resistance levels and accentuated geographical separation. Accordingly, the study of these strains could provide an insight into the intraspecific variation in metal(loid) detoxification mechanisms of a unique acidophilic basidiomycetous yeast species.

2. Objectives

The main goal in this work consisted in unveiling heavy metal(loid) resistance mechanisms in two strains from the unique acidophilic yeast *Cryptococcus* sp.. To achieve this main goal, intermediary aims were established and studied by applying the following approaches:

A. Physiological approach to assess the influence of sulfate availability on heavy metal(loid) resistance.

   As mentioned before, sulfur metabolism appears to play a central role in metal(loid)-induced response. Also, this subject is of particular importance since high sulfur/sulfate concentrations were detected in the natural habitats of the two chosen strains.

B. Cytological approach to evaluate the involvement of thiolated peptides in metal(loid) detoxification mechanisms.

   Since the thiol groups present in Cys side chains are often involved in metal(loid) detoxification in yeasts, the possibility of accumulation of thiolated peptides in response to metal(loid) exposure was assessed in optimal sulfate conditions, determined in the physiological approach.

C. Molecular approach to identify genes and gene products involved in metal(loid) detoxification mechanisms.

   Gene homologues of transporters involved in metal(loid) detoxification were identified in the type species of the *Cryptococcus* genus, *C. neoformans*. The presence of homologues of these genes was evaluated in the genome of both selected *Cryptococcus* sp. strains.

   Gene products associated with a Cd-induced response were analyzed at a molecular level. To do so, a transcriptomic approach was conducted by applying suppression subtractive hybridization.

3. Experimental workflow

The following illustration represents the experimental workflow conducted in the present work.

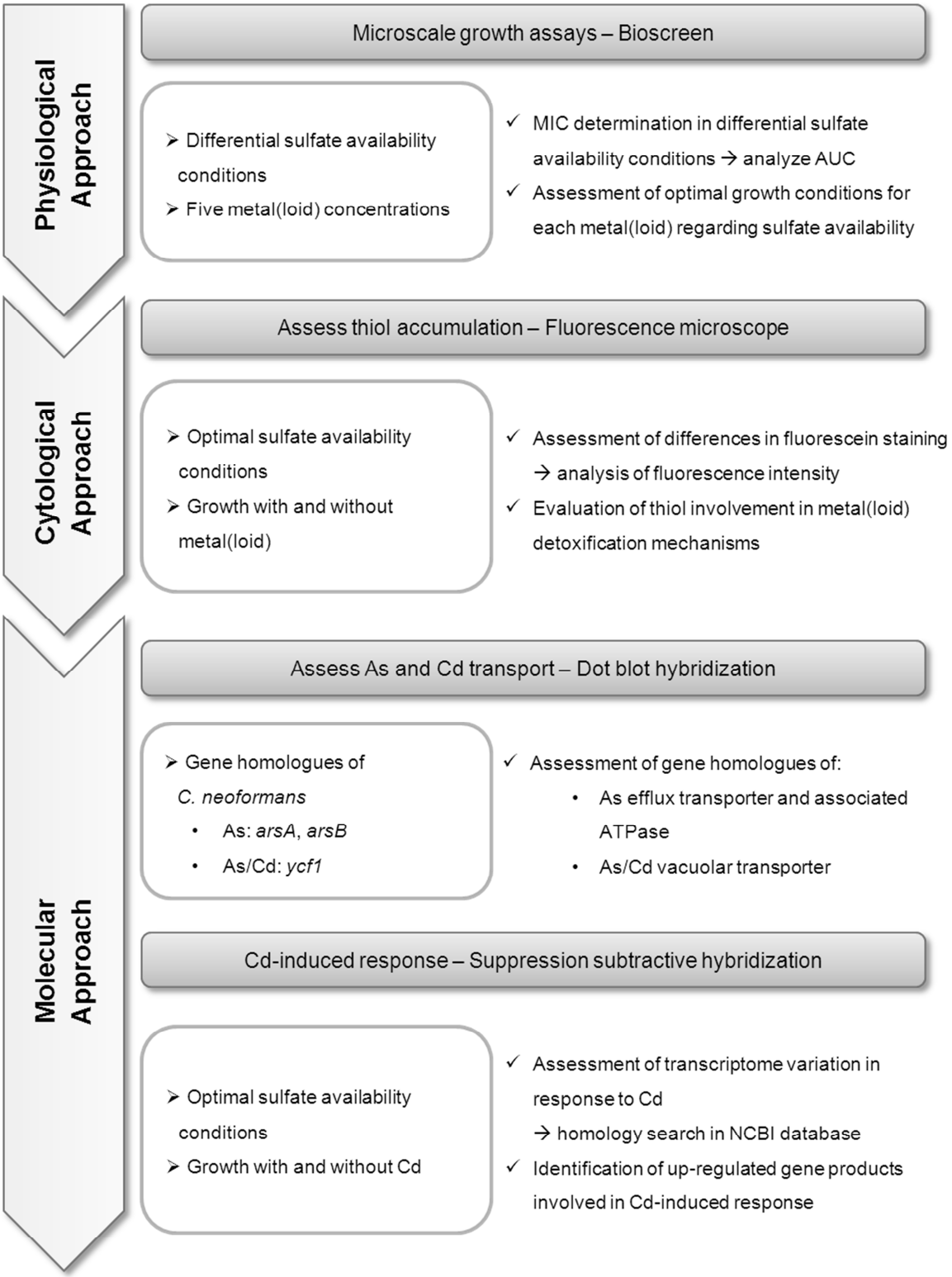

4. General methodologies

Strains and growth conditions

Two strains of *Cryptococcus* sp. were studied in this work: MSD44 and CRUB1564. Both are considered acidophilic (optimum pH for growth 2.5-4) and were maintained in acidic (pH=3) solid Malt Yeast Peptone (MYP; composition and preparation in Annex I) growth medium. Microbiological experiments with these strains were performed with cells grown in MYP medium at room temperature (RT) for three days.

The *Saccharomyces cerevisiae* strain used in the present work belongs to the Yeast Portuguese Culture Collection (PYC3507). This strain was maintained in MYP media (pH=5-5.5) and incubated overnight at 30ºC to obtain biomass for microbiological assays. The same incubation conditions were applied for *Cryptococcus neoformans*, provided by the Instituto de Higiene e Medicina Tropical.

Liquid Yeast Nitrogen Base (YNB; composition and preparation in Annex II) was used in several assays and it was prepared in two variants: Sulfate-YNB and Chloride-YNB, when the added ammonium salt was ammonium sulfate or ammonium chloride, respectively. For the acidophilic strains, the pH of the media was adjusted to 3.0 with H_2SO_4, and incubation occurred at RT. For the neutrophilic strains, the pH of the media was adjusted to 5-5.5 and yeast cells were incubated at 30ºC. Medium agitation was kept constant throughout the incubation periods.

Heavy metal(loid) solutions

In the present study, two chemical forms of each metal(loid) were tested: As was tested as As(V) and As(III); Cd, Cu and Zn were tested as metal sulfate and metal chloride.

As(V) ($(Na_2HAsO_4)\cdot 7H_2O$), As(III) ($NaAsO_2$), Cd sulfate ($3(CdSO_4)\cdot 8H_2O$) and chloride ($CdCl_2$), Cu sulfate ($CuSO_4\cdot 5H_2O$) and chloride ($CuCl_2\cdot 2H_2O$), Zn sulfate ($ZnSO_4\cdot 7H_2O$) and chloride ($ZnCl_2$) stock solutions were prepared by adding sterilized ultra-pure water (supw) to the respective metal(loid) conjugates and adjusting pH to 3.0 with H_2SO_4.

The solutions were then sterilized by filtration with syringe filters (with a pore diameter of 0.22 µm) and stored in falcon tubes at RT.

5. Physiological approach

Determination of minimal inhibitory concentration in differential sulfate availability conditions

Microscale growth assays were conducted to establish minimal inhibitory concentrations (MIC) of the four tested metal(loid)s in different conditions of sulfate availability. These assays were performed using 10 by 10 well honeycomb sterile plates containing a working volume of 300 µL per well. Microbial growth was monitored with the automated turbidimeter Microbiology Reader Bioscreen C (Growth Curves USA, New Jersey, USA; Begot *et al.*, 1996).

In these metal(loid) resistance assays, five concentrations of each metal(loid) were tested in 2-fold dilution series, from 1:2 to 1:32. These dilution series and corresponding metal(loid) concentrations are shown in Table 3. Liquid YNB medium was used in these assays, in two variants: Sulfate-YNB and Chloride-YNB. These two YNB media were combined with two chemical forms/salts of each metal(loid): As(V) *vs.* As(III) for As, and metal sulfate *vs.* metal chloride for all other metals. As a result, two sulfate availability conditions were tested for As, and four were tested for the other metals, for each strain. A schematic representation for the Cd resistance assay is depicted in Figure 4. The same principle was applied to the other metal(loid)s under study.

Table 3 Two-fold metal(loid) concentrations tested in metal(loid) resistance assays. Concentrations are given in mM and denote metal(loid) concentration, not the metal salt.

	1:2	**1:4**	**1:8**	**1:16**	**1:32**
As	17	8.5	4.3	2.1	1.1
Cd	54.5	27.3	13.6	6.8	3.4
Cu	54.2	27.1	13.6	6.8	3.4
Zn	230	115	57.5	28.8	14.4

Each assay included adequate metal(loid)-free controls. A negative control (Cneg) with supw and medium, without inoculum, was used to ensure there were no contaminants in the medium. A positive control (Cpos) with supw and medium, with inoculum, was used to ensure inoculum viability. After medium preparation in each well, a cell suspension with OD_{600}=0.9 U (equivalent to $9x10^6$ cells mL^{-1}) was prepared for each strain. With the exception of Cneg controls, each well was inoculated with 1 µL from this suspension using a calibrated inoculation loop, which corresponded to approximately $9x10^3$ cells.

Parameters for growth assays were set in Bioscreen C software Research Express (Transgalactic Ltd, Helsinki, Finland). The microplates were incubated at 22ºC with a pre-heating step of 10 minutes, with continuous and intensive shaking. The corrected optical density (ODc, where the first OD measurement is considered 0.001 U) was measured for each well, every two hours for 5 days, with a wide band filter to determine turbidity, resulting in 60 OD measurements per well.

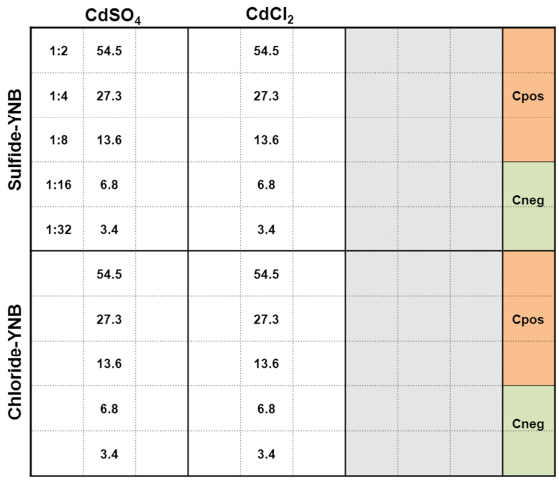

Figure 4 Schematic representation of the Cd resistance assay for one strain. Each square represents one well in the 10 by 10 honeycomb plate. Each metal concentration was tested in triplicate for each sulfate availability condition, resulting in 3x20 determinations per metal, per strain. The depicted Cd concentrations refer to the metal ion, not the metal salt. 1:2 to 1:32 relates to the metal dilution series performed in each well. Controls were performed at least in duplicate. Cpos corresponds to the positive control, containing supw and medium, with inoculum. Cneg corresponds to the negative control, containing supw and medium, without inoculum.

Data analysis

The parameter area under the curve represents ODc as a function of time and was determined automatically for each well by the Research Express software. Data for AUC for all wells was exported to an Excel working sheet (Microsoft Software) and analyzed for each condition (AUCx) as follows:

$$AUCx = \frac{Average\ AUC}{Average\ AUC\ Cpos} - Average\ AUC\ Cneg$$

The average Cneg value for each YNB medium was used as a correction factor, to subtract the background in microbial growth readings. The average Cpos value for each YNB medium was used as a normalization factor in data analysis, to allow comparison between assays. As a result, AUCx represents the corrected normalized average AUC for each condition (n=3). The threshold for positive growth was established at AUCx ≥ 0.05 (i.e., 5% of the average growth of the Cpos), as it presented a good correspondence with visible growth on the microplate (data not shown) and with maximum ODc ≥ 0.1 (ODc threshold previously established by Gadanho, M., personal communication).

MIC was defined as the lowest metal(loid) concentration tested in which AUCx < 0.05. Accordingly, the maximum tolerated concentration determined by *m*icroscale assays, *m*MTC, was obtained. This concentration corresponds to the one immediately below MIC, i.e., the highest metal(loid)

concentration tested that allowed detectable growth (AUCx ≥ 0.05). To assess the influence of sulfate availability on resistance to each metal(loid), yeast growth was statistically analyzed by comparing AUCx values at the *m*MTCs in the four sulfate availability conditions.

First, F-test was applied to determine homocedasticity. Then, a t-Student test was performed, considering a confidence level of 95%, assuming equal or unequal variances, depending on F-test results (Zar, 1999). For each strain and for each metal(loid), comparisons were performed between average AUCx for the *m*MTC determined in: (i) Sulfate-YNB *vs.* Chloride-YNB and (ii) As(V) *vs.* As(III) or metal sulfate *vs.* metal chloride within the same YNB variant.

Results and discussion

The determined MIC, *m*MTC and corresponding AUCx values are displayed in Table 4. MIC determinations are also represented in Figure 5.

Table 4 Minimal inhibitory concentrations (MIC), maximum tolerated concentrations (*m*MTC) and corresponding AUCx values, determined with Bioscreen C turbidimeter. $+SO_4$ and $–SO_4$ refer to the type of YNB medium: Sulfate-YNB and Chloride-YNB, respectively. Metal(loid) concentrations are given in mM.

	MIC (mM)				***m*MTC (mM)**				**AUCx in *m*MTC**			
	MSD44		**CRUB1564**		**MSD44**		**CRUB1564**		**MSD44**		**CRUB1564**	
	$+SO_4$	**$-SO_4$**	**$+SO_4$**	**$-SO_4$**	**$+SO_4$**	**$-SO_4$**	**$+SO_4$**	**$-SO_4$**	**$+SO_4$**	**$-SO_4$**	**$+SO_4$**	**$-SO_4$**
As(V)	17	17	17	17	8.5	8.5	8.5	8.5	0.60	0.52	0.87	0.64
As(III)	8.5	8.5	8.5	8.5	4.3	4.3	4.3	4.3	0.93	0.99	0.83	1.04
$CdSO_4$	54.5†	54.5†	54.5†	54.5†	54.5	54.5	54.5	54.5	0.23	0.31	0.10	0.10
$CdCl_2$	54.5†	54.5†	54.5†	54.5	54.5	54.5	54.5	27.3	0.25	0.23	0.09	0.19
$CuSO_4$	54.2	27.1	6.8	3.4¥	27.1	13.6	3.4	3.4	0.25	0.33	0.38	0.01
$CuCl_2$	27.1	27.1	6.8	3.4¥	13.6	13.6	3.4	3.4	0.42	0.26	0.44	0.00
$ZnSO_4$	230†	230	230	115	230	115	115	57.5	0.13	0.14	0.10	0.18
$ZnCl_2$	230	115	115	115	115	57.5	57.5	57.5	0.14	0.41	0.24	0.18

†The real MIC for the corresponding metals was not determined, as the corresponding strains presented AUCx > 0.05 for the highest metal concentration tested.

¥AUCx < 0.05 for all tested metal concentrations for the corresponding strain.

As showed in Figure 5A, results for the microscale growth assays with As show that the MIC values for As(V) are higher than those presented for As(III) in both strains. This result is in accordance with the previously described higher toxicity of As(III) (Oremland & Stolz, 2003).

Statistical assessment of average growth upon exposure to different As chemical forms showed that the average growth obtained in the corresponding *m*MTCs is equivalent (Table 4). The same

result was obtained upon comparison of average growth in Sulfate-YNB *vs.* Chloride-YNB media. The latter result suggests that As resistance is not influenced by sulfate availability in either strain.

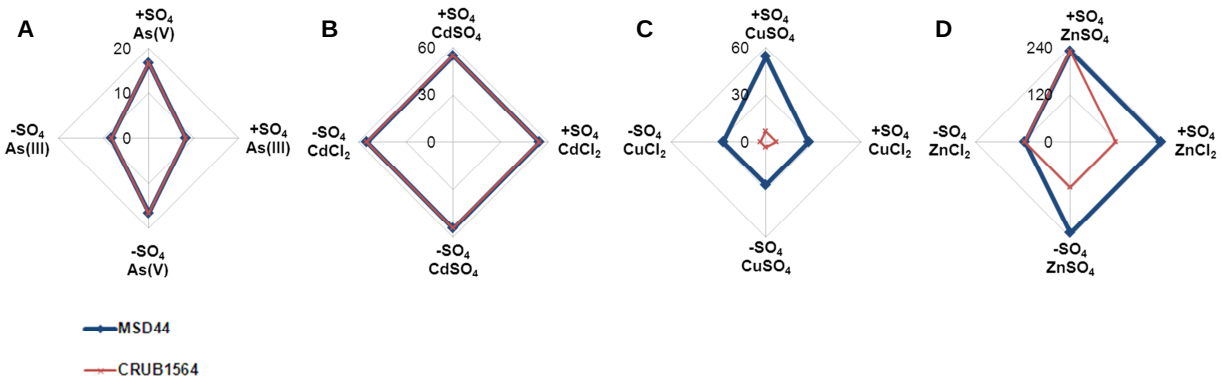

Figure 5 Representation of MIC determination results for MSD44 and CRUB1564, for As, Cd, Cu and Zn in different sulfate availability conditions: with Sulfate-YNB ($+SO_4$) and with Chloride-YNB ($-SO_4$). For each YNB medium, two chemical forms of each metal(loid) were tested. The values next to the axis represent metal(loid) concentration in mM.

Results for microscale growth in the presence of Cd (Figure 5B) showed that the Cd MIC was the same in both strains (54.5 mM; Table 4) in all tested sulfate availability conditions. However, statistical analysis of average growth within the obtained *m*MTC revealed that CRUB1564 reaches higher AUCx in Chloride-YNB medium in the presence of $CdSO_4$ when compared to growth with Sulfate-YNB (p=0.005; Table 4).

MIC determination for Cu (Figure 5C) shows an overall higher level of resistance for MSD44 than for the Argentinean strain. In fact, there was no detectable growth for CRUB1564 in Chloride-YNB (Table 4). This result suggests a sulfate dependency and will be analyzed further in detail.

Statistical analysis of growth in the presence of $CuSO_4$ revealed that sulfate availability influences the growth of MSD44, since AUCx was higher in Sulfate-YNB medium (Table 4; p=0.012).

Finally, average growth in the presence of Zn (Table 4) was statistically analyzed. For this metal, the results showed that MSD44 reaches higher AUCx in the presence of Sulfate-YNB, regardless of the metal chemical form (p=0.002 for $ZnSO_4$ and for $ZnCl_2$).

To understand the apparent sulfate dependence for Cu resistance in the Argentinean strain, two additional microscale growth assays were performed. In these assays, four Cu concentrations were tested: as described above, with metal dilutions from 27.1 to 3.4 mM (Table 3).

The first assay was conducted in order to evaluate the yeast response to increasing concentrations of sulfate, by assessing the minimum sulfate concentration necessary to obtain growth. To achieve this goal, sulfate in $MgSO_4$ form was added to the metal-containing medium in three concentrations (mM): 520, 416 and 312, where the first concentration (520 mM) corresponds to the sulfate concentration present in Sulfate-YNB medium.

A second assay was performed to understand whether the addition of magnesium (Mg) to the medium influenced growth. Three Mg concentrations (as $MgCl_2$) were tested with the same Cu concentrations tested before (27.1 to 3.4 mM). The Mg concentrations used in this assay were equivalent to the Mg concentrations added in the assay with $MgSO_4$.

Results from these additional assays are presented in Table 5 and Figure 6.

Table 5 Minimal inhibitory concentrations (MIC), maximum tolerated concentrations (*m*MTC) and corresponding AUCx values for the two additional microscale growth assays, determined with Bioscreen C turbidimeter. $MgSO_4$ and $MgCl_2$ refer to what was being tested in the additional microscale growth assay: different sulfate concentrations and different magnesium concentrations, respectively. Concentrations are given in mM.

	MIC (mM)						***m*MTC (mM)**						**AUCx in *m*MTC**					
	$MgSO_4$			**$MgCl_2$**			**$MgSO_4$**			**$MgCl_2$**			**$MgSO_4$**			**$MgCl_2$**		
	520	**416**	**312**	**520**	**416**	**312**	**520**	**416**	**312**	**520**	**416**	**312**	**520**	**416**	**312**	**520**	**416**	**312**
$CuSO_4$	27.1	27.1[†]	27.1[†]	3.4[¥]	3.4[¥]	6.8	13.6	13.6	13.6	3.4	3.4	3.4	0.35	0.40	0.41	0.00	0.03	0.12
$CuCl_2$	27.1[†]	27.1[†]	27.1[†]	3.4[¥]	3.4[¥]	3.4[¥]	13.6	13.6	13.6	3.4	3.4	3.4	0.32	0.41	0.27	0.00	0.03	0.03

[†]The real MIC for the corresponding metals was not determined, as the corresponding strains presented AUCx > 0.05 for the highest metal concentration tested.

[¥]AUCx < 0.05 for all tested metal concentrations for the corresponding strain.

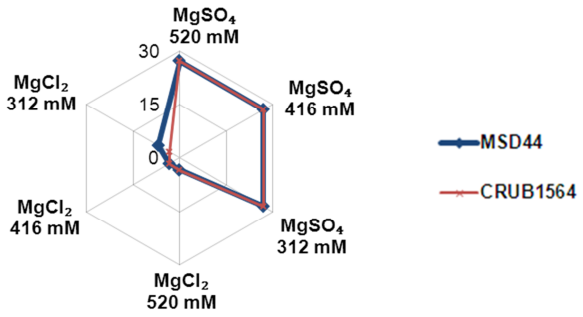

Figure 6 Results of MIC determination for CRUB1564 with Cu in Chloride-YNB medium supplemented with different sulfate (as $MgSO_4$) and Mg concentrations (as $MgCl_2$). The values next to the axis represent Cu concentration in mM.

Although the minimum sulfate concentration necessary to ensure yeast growth upon exposure to Cu was not determined with these assays, the MICs obtained clearly show that the addition of sulfate as $MgSO_4$ to Chloride-YNB medium allows CRUB1564 to grow in the presence of this metal (Figure 6). Statistical analysis of AUCx in the *m*MTCs (Table 5) showed that average growth with $CuSO_4$ was equivalent in the three sulfate concentrations tested. However, for $CuCl_2$, the average growth was significantly reduced in the lowest sulfate concentration tested (312 mM; p=0.048), which also reflects an influence of sulfate availability.

In the case of the microscale growth assay testing different Mg concentrations, detectable growth (AUCx>5%) was only observed for the condition with 3.4 mM of $CuSO_4$ and 312 mM of $MgCl_2$ (Table 5). Statistical analysis showed that growth in this condition is much lower than for $CuSO_4$ with 312 mM of $MgSO_4$ (p=0.007), suggesting that sulfate was necessary for the higher MIC values observed in the first additional assay.

Considering the results obtained in these additional assays, Cu resistance in CRUB1564 was clearly influenced by sulfate (as $MgSO_4$) availability. MIC values for $CuSO_4$ resistance increased from 6.8 mM with Sulfate-YNB (Table 4 and Figure 5C) to 27.1 with the same theoretical sulfate concentration (520 mM; Table 5 and Figure 6). This suggests that the addition of sulfate may not have been the only factor responsible for the improved Cu resistance, as a synergistic effect of Mg and sulfate could be taking place. The possibility of Mg participation on Cu resistance in this strain was not further assessed in the present study.

In summary, this physiological approach allowed assessment of the influence of sulfate in metal(loid) resistance for both acidophilic strains. AUCx analysis showed that the sulfate availability positively influences the Portuguese strain's resistance to Cu, when added as $CuSO_4$, and Zn in both metal forms. A different outcome was observed for the Argentinean strain for $CdSO_4$ resistance, since growth was enhanced when sulfate was absent from the YNB growth medium. CRUB1564 showed, however, sulfate dependency for Cu resistance, as this strain does not present detectable growth upon expose to Cu unless sulfate is provided in the medium, as Sulfate-YNB or as $MgSO_4$. Overall, the obtained results suggest that sulfur availability, as sulfate, plays a role in resistance to some of the tested metal(loid)s.

In the following cytological approach, the participation of thiolated peptides in metal(loid) response will be assessed. As mentioned in the Introduction section, these peptides possess Cys residues which have sulfur in the thiol (GS) groups. As a consequence, analysis of the variation of intracellular thiol content should allow further enlightenment on the role that sulfur plays in metal(loid) detoxification.

Adjustment of growth conditions for cytological and molecular approaches

To proceed to the cytological and molecular approaches in this study, it was necessary to obtain a large amount of biomass to successfully conduct the experiments. Accordingly, the conditions used for yeast growth were optimized.

Overall, the results from the microscale growth assays showed that the growth conditions with the highest sulfate concentrations allowed better microbial growth. In accordance with these results, the YNB medium used in subsequent approaches was Sulfate-YNB and the metal chemical form was the metal sulfate. In the case of As, the chemical form As(V) was used since it presented itself as being less toxic than the trivalent form.

Yeast growth cultures were produced in 5 mL volumes and the inoculum was optimized in order to obtain a sufficient amount of biomass in a short period of time. Accordingly, the inoculum for 5 mL of growth culture was established at $1.5x10^7$ cells mL^{-1}, which corresponded to a OD_{600}=1.5 U. The growth conditions were as stated in the General methodologies section.

Finally, the metal(loid) concentrations used for yeast growth were also optimized. This was necessary since the metal(loid) concentrations that allowed detectable growth in microscale assays (*m*MTC; AUC$_x$>5%) were too elevated to allow sufficient biomass for the execution of cytological and molecular experiments. Several growth assays were then conducted to determine the maximum tolerated concentrations of the metal(loid)s in these scale up conditions (*su*MTC). These assays were performed with both acidophilic strains and with *S. cerevisiae*, since this model yeast was used as a control in cytological experiments. The results for the obtained *su*MTCs are listed in Table 6.

Table 6 Maximum tolerated concentrations determined in *s*cale *u*p growth assays (*su*MTC) with Sulfate-YNB medium (pH=3 for MSD44 and CRUB1564; pH=5 for *S. cerevisiae*). The depicted concentrations, given in mM, refer to concentration of the metal(loid) (As, Cd, Cu and Zn), not the metal salt.

	MSD44	**CRUB1564**	***S. cerevisiae***
As(V)	4.3	8.5	n. d.
$CdSO_4$	27.3	13.6	0.2
$CuSO_4$	6.8	3.4	n. d.
$ZnSO_4$	28.8	28.8	n. d.

n. d. – not determined.

6. Cytological approach

Protocol optimization and sample preparation

The hypothesis of thiol accumulation in response to the presence of metal(loid)s was evaluated in MSD44 and CRUB1564 cells using the fluorescent CellTracker Green CMFDA (5-chloromethylfluorescein-diacetate) probe from Invitrogen (California, USA). This reagent passes freely through membranes and, once inside the cell, is cleaved by nonspecific esterases. The chloromethyl group of CMFDA reacts with thiol groups in thiolated peptides and the resulting dye-protein conjugate is cell-impermeant. Additionally, the excess unconjugated dye exits the cell by passive diffusion. To assess the possibility of thiol accumulation in response to metal(loid)s, the CMFDA fluorescence intensity observed for cells grown in the presence of the metal(loid) was compared to the intensity for cells grown without metal (control condition).

The protocol for sample preparation and staining was adapted and optimized from the Invitrogen CellTracker manual for Probes for Long-Term Tracing of Living Cells. Considering the lack of information on settings for this protocol in yeasts, three parameters were optimized: (i) initial inoculum, (ii) CMFDA concentration, and (iii) CMFDA incubation time. Optimization was conducted using *S. cerevisiae* as a control, grown with and without Cd. This model yeast was used with Cd since it is described in the literature as accumulating thiolated peptides in response to exposure to this metal (reviewed in Tamás & Wysocki, 2010). After optimization, a control using *S. cerevisiae* cells was performed in all assays as an experimental control to ensure the success of the experimental protocol.

The optimized protocol was performed as follows: yeast growth obtained in scale up conditions with and without metal(loid) was harvested in exponential phase by centrifugation (5 min at 4000 rpm). $2x10^6$ of these cells were then transferred to 15 mL falcon tubes containing 1 µM CMFDA in Sulfate-YNB (final volume 2 mL) and incubated for 25 min. The incubation conditions used for incubation periods in this protocol were the same as those applied for yeast growth (see General methodologies).

From this point forward, all samples were protected from light. After CMFDA incubation, the cells were harvested by centrifugation (10 min at 4000 rpm), ressuspended in fresh Sulfate-YNB medium without CMFDA and without metal(loid)s, and incubated for 30 min. Then, the samples were washed with phosphate saline buffer (PBS; 5 min, 4000 rpm) and fixed with 3.7% formaldehyde prepared in PBS (30 min; 100 rpm) to crosslink the amines in peptides-dye conjugates. After washing twice with PBS, the cells were ressuspended in 200 µL PBS and transferred to 1.5 mL eppendorf tubes. Afterwards, 10 µL aliquots were placed on microscope glass slides and allowed to dry for 30 min at 37ºC. A drop of an antifade reagent (Molecular Probes ProLong Gold antifade reagent, Invitrogen, California, USA) was added on top of the dried sample. Finally, a cover slip was placed on top of the samples.

The samples were observed in an inverted fluorescence microscope (Olympus IX50) considering the absorption and emission wave lengths indicated for CMFDA: 492 nm (blue) and 517 nm (green), respectively. Images were captured with the Sensicam PCO camera with an exposure time of 0.4 seconds using the software Image-Pro Plus Version 6.0 (Media Cybernetics, Inc, Maryland, USA).

Data analysis

The fluorescence intensity of each pair of control *vs.* presence of metal(loid) conditions was compared. For each condition, the fluorescence intensity of the highest possible number of cells was measured to provide accurate mean fluorescence intensity values. Consequently, sample sizes (n) were different for each condition and are listed in Table 7.

Table 7 Sample sizes (n) for MSD44 and CRUB1564 in cytological assays for all tested conditions.

	Control sample size	Metal(loid) and sample size
MSD44	52	As(V), n=113; $CuSO_4$ n=404
	260	$CdSO_4$, n=619
	73	$ZnSO_4$, n=199
CRUB1564	129	As(V), n=360; $CuSO_4$ n=609
	199	$CdSO_4$, n=253; $ZnSO_4$, n=415

Relative fluorescence intensity (RFI) for the tested conditions was calculated as:

$$RFI = \frac{Average\ fluorescence\ intensity\ for\ cells\ in\ each\ condition}{Average\ fluorescence\ intensity\ for\ control\ cells}$$

As a consequence, RFI for control conditions was always 1, and >0 for presence of metal(loid) conditions. The RFI values for each pair of control *vs.* presence of metal(loid) conditions were statistically analyzed. First, a F-test was performed to assess homocedasticity, and then a t-Student test was applied considering a confidence level of 95%, assuming equal or unequal variances, depending on F-test results (Zar, 1999). Additionally, a confidence interval with a 95% confidence level was obtained for each RFI value.

Results and discussion

Thiol probing results for all tested metal(loid)s in optimal sulfate availability conditions, and corresponding RFI values, are displayed in Figure 7A and 7B, respectively.

The images captured for CMFDA staining with and without As(V) clearly showed a differential staining for the Portuguese strain, but not for the Argentinean one (Figure 7A, As(V)). These observations are supported by the RFI values: 1.36 for MSD44 with As, and 0.96 for CRUB1564 with As (Figure 7B, As(V)).

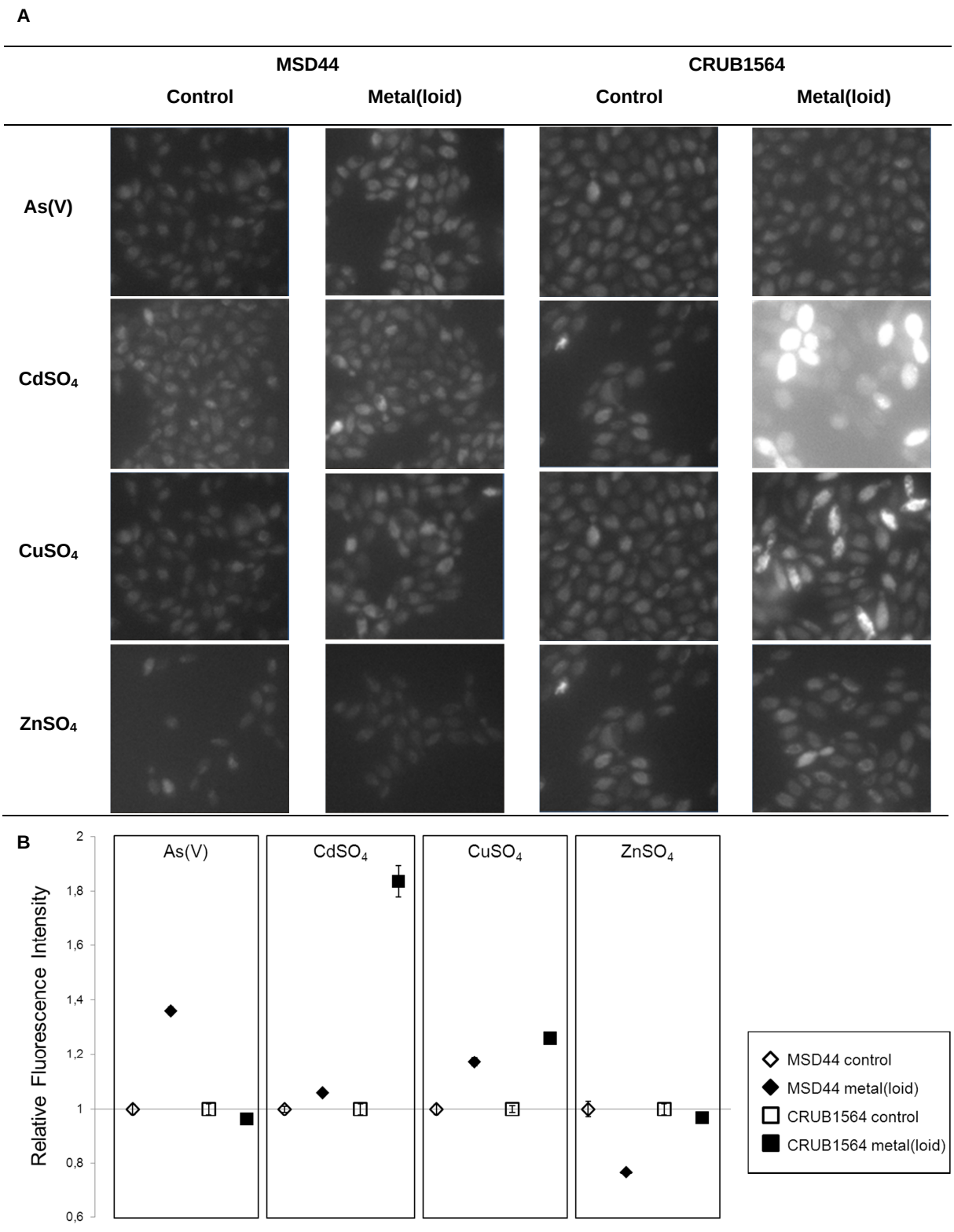

Figure 7 Results for the cytological assays for the acidophilic strains MSD44 and CRUB1564, with and without metal(loid)s. **A** Images obtained for CMFDA staining in control *vs.* presence of metal(loid) conditions. Samples were observed under the fluorescence microscope (Olympus IX50) with 100x magnification. Images were captured with (Sensicam PCO) using the software Image-Pro Plus Version 6.0 (Media Cybernetics, Inc, Maryland, USA). All images were adjusted using the same software, by applying a display range of fluorescence intensity from 150 to 750 units. **B** RFI values for control *vs.* presence of metal(loid) conditions for MSD44 and CRUB1564. The error bars represent confidence intervals with a 95% confidence level.

Upon statistical analysis of RFI values, the difference in fluorescence intensity was significant for MSD44 (p=2.86E-56). Accordingly, results point to an As-induced response in this strain that consists in intracellular accumulation of thiolated peptides. For the Argentinean strain, the obtained results show that thiol accumulation does not change in the presence of As (Figure 7). However, the statistical analysis provided a p-value of 0.003, which, although considered significant at the applied confidence level, is much higher than that obtained for a clearly significant differential staining (p=2.86E-56 for MSD44). This statistically significant difference in RFI values for CRUB1564 may be attributed to a very small variation in average fluorescence intensity (<0.014; data not shown) and, as a consequence, a variation of 0.04 (i.e., 4%) in RFI is considered statistically significant. As a consequence of the abovementioned considerations, the fluorescence intensity in the presence of As was considered to be similar to that of the control condition for CRUB1564.

The results for CMFDA staining for control *vs.* Cd staining show a differential staining for the Argentinean strain, but not for the Portuguese strain (Figure 7A, $CdSO_4$). This difference is reflected in the obtained RFI values: 1.83 for CRUB1564, and 1.06 for MSD44 (Figure 7B, $CdSO_4$). Statistical analysis of these results confirmed the significant differences observed for CRUB1564 (p=2.49E-83). For MSD44, statistical analysis provided a p-value of 2.18E-8. For the same reasons as presented above for the statistical analysis for CRUB1564 in the presence of As, the intracellular thiol content upon exposure to Cd for MSD44 was considered equivalent to the control condition.

For Cu, results for CMFDA staining suggest thiol accumulation for both strains (Figure 7A, $CuSO_4$). Statistical analysis of RFI values confirmed the observed differential staining: RFI=1.17 for MSD44 (p=4.54E-16), and RFI=1.26 for CRUB1564 (p=9.04E-56) in the presence of Cu (Figure 7B, $CuSO_4$).

Finally, neither strain showed thiol accumulation upon exposure to Zn (Figure 7A, $ZnSO_4$). In fact, a decrease in fluorescence intensity was observed in the Portuguese strain in the presence of Zn. Statistical analysis for RFI in MSD44 (RFI=0.77; Figure 7B, $ZnSO_4$) confirmed the significance of this decrease in fluorescence intensity (p=8.86E-25). For the Argentinean strain, statistical analysis of RFI values (RFI=0.97) provided a p-value of 0.008 which, as justified before, was considered as not having biological significance.

In summary, results for the cytological approach for MSD44 point to a thiol accumulation in response to As and Cu. However, upon exposure to Zn, the thiol pool is diminished. For the Argentinean strain, the results obtained with this approach show that the heavy metals Cd and Cu lead to thiol accumulation.

Considering the contrasting results between strains for the nonessential metal(loid)s As and Cd, and taking into account the available information on detoxification mechanisms for these elements, a series of experiments involving molecular approaches were designed and conducted.

7. Molecular approach

7.1. Metal(loid) transporters

To further comprehend metal(loid) detoxification mechanisms in the acidophilic yeasts at study, the presence of homologues involved in these mechanisms was assessed *in silico* in basidiomycetous yeasts. To do so, the sequences of proteins involved in metal(loid) detoxification, from the original microbes, were used as a protein query in a search in a non-redundant protein database (blastp; Altschul *et al.*, 1990) in National Center for Biotechnology Information (NCBI), using the default settings. Gene homologues of transporters involved in As and Cd detoxification were identified in the genome of *C. neoformans*, the type species of the genus. These transporters include the As(III) efflux transporter complex ArsAB (Tsai *et al.*, 2009) and the vacuolar transporter Ycf1 (see Introduction).

The As(III) efflux mechanism conducted by the ArsAB pump was first identified and described in bacteria and is constituted by two components: the actual As(III) pump (ArsB) and an optional ATPase (ArsA). According to the available literature, ArsB is able to confer As(III) resistance by itself, however, when ArsA is co-expressed, the ArsAB pump transports As(III) more efficiently (reviewed in Tsai *et al.*, 2009). The genes found in *C. neoformans* present homologies with ArsA (accession number XM_767623.1) and ArsB (XM_569061.1) described in the bacterial *ars* operon, and were not homologues of genes in other yeasts (information available in NCBI database). Considering the results obtained for As detoxification with the previous approaches, the possibility of As(III) efflux should be evaluated. As mentioned in the Introduction section, Ycf1 transports $As(GS)_3$ and $Cd(GS)_2$ conjugates to the vacuole, and was first described in *S. cerevisiae* (Li *et al.*, 1997; Prévéral *et al.*, 2006). Since thiolated peptides appear to be involved in As and Cd detoxification for MSD44 and CRUB1564, respectively, the search for evidence of the presence of this transporter (accession number XM_569810.1) is of great importance in both strains.

Homology for the As(III) transporter Arr3 (see Introduction) was also found in *C. neoformans* (in NCBI database; accession number XP_772635.1). This transporter is implied in As(III) detoxification in model yeasts, which are not related with very high resistance levels (see Introduction). Accordingly, its presence by homology search was not assessed in the genome of the acidophilic strains.

Considering this information, the first molecular approached applied aimed to assess the presence of *arsA*, *arsB* and *ycf1* gene homologues, found in *C. neoformans*, in the genomes of the acidophilic strains MSD44 and CRUB1564.

DNA extraction and sample preparation

Homologue gene search was conducted to assess the presence of homologue genes of metal(loid) transporters in the genomes of MSD44 and CRUB1564. To do so, DNA was extracted from both acidophilic strains and from the neutrophilic yeasts *C. neoformans* and *S. cerevisiae* to use as controls during the experiments.

DNA extraction was conducted according to the following protocol: cells grown in solid MYP medium (see General methodologies) were recovered into an eppendorf tube containing Tris EDTA Buffer (TE, 1 mL) and washed by centrifugation (5 min, 4000 rpm). After ressuspending in Lysis Buffer (composition in Annex III) and adding approximately 200 µL of glass beads (acid-washed 425-600 µm glass beads, Sigma-Aldrich, Missouri, USA), cells were lysed by vortexing for 2 min at maximum speed. The samples were then incubated for 1 hr at 65ºC and further lysed by repeating the vortexing step. Proteins were removed by phenol extraction (1x vol; 10 min, RT, 13000 rpm) followed by a chloroform-isoamyl alcohol 24:1 purification (1x vol; 10 min, RT, 13000 rpm). The aqueous phase was transferred to a new eppendorf tube and nucleic acid was precipitated with salt (NaAc, 0.3 M final concentration) and cold absolute ethanol (-20ºC, 2.5x vol) on ice for 30 min. The resulting pellet was washed with cold 70% ethanol (1 mL). Finally, the extracted nucleic acid was ressuspended in PCR grade water and treated with RNase (working concentration 50 µg mL^{-1}) overnight at 4ºC.

DNA quality was determined by gel electrophoresis of the DNA extracts (5 µL from each sample), using 1% agarose and TBE buffer (0.5x). DNA quantification was assessed by a fluorescence-based method using Qubit dsDNA High Specificity Assay Kit, according to the manufacturer's recommendations, with Qubit fluorometer (Invitrogen, California, USA).

Probe synthesis by PCR

To assess the presence of the mentioned homologue genes in the genomes of the acidophilic strains MSD44 and CRUB1564, three DNA probes were synthesized by PCR. The resulting PCR products corresponded to homologue genes identified in *C. neoformans* as being involved in metal(loid) detoxification by transport: *arsA*, *arsB* and *ycf1*.

To produce these probes, forward and reverse primers were designed with Primer-BLAST, a tool in NCBI, according to the available sequences. The conditions for PCR amplification were optimized for each primer set and the optimized settings are displayed in Table 8.

After amplification, the resulting PCR products were purified using the Jetquick PCR product Purification Spin Kit (Genomed GmbH, Germany), according to the manufacturer's instructions, and sequenced using the laboratory sequencing services. The resulting sequences were submitted to a visual correction with Chromas Lite 2.01 software (Technelysium Pty, Australia) and used as a

nucleotide query in a search in nucleotide databases (blastn) in NCBI, using the default settings. The results of this search confirmed that the three PCR products corresponded to the gene homologues at study.

Table 8 Optimized settings for PCR amplification of *arsA*, *arsB* and *ycf1* in *C. neoformans*.

Temperature (ºC)	Time (min)	Number of cycles
94	3	1
94	1	34
65	1	
72	1	
72	3	1

The homology search for the three mentioned genes was first conducted by PCR amplification in the genomic DNA of MSD44 and CRUB1564, with the forward and reverse primers described above. However, this approach resulted in amplification of unrelated products, even using different annealing temperatures (data not shown), which could be attributed to sequence differences between the type species and the tested strains of *Cryptococcus* sp.. As a consequence, dot blot hybridization was performed to search for gene homologues in the acidophilic strains.

The probes for dot blot hybridization were synthesized by PCR, using the abovementioned primer sets and amplification settings (Table 8), according to the PCR DIG-labeling Mix protocol from Roche (Mannheim, Germany). The DIG-labeling mix contains DIG-conjugated dUTPs that are incorporated into the PCR products as the PCR takes place. Accordingly, the resulting PCR products correspond to DIG-labeled probes, containing DIG-dUTPs.

Dot blot hybridization

For this approach, positively charged nylon membranes were used (from Roche Diagnostics, Mannheim, Germany). One membrane for each probe was prepared by adding dots of yeast DNA (5 µL per dot), from *C. neoformans*, MSD44, CRUB1564 and *S. cerevisiae*, as represented in Figure 8. DNA from the type species *C. neoformans* was used as control for the presence of the homologue gene.

The amount of DNA present in each dot was normalized according to the genome size of the tested yeasts, in an effort to ensure the same number of genome copies in the different dots. However, since this information is not available for the acidophilic strains, the genome size was assumed to be approximately the same as the type species *C. neoformans* (Table 9).

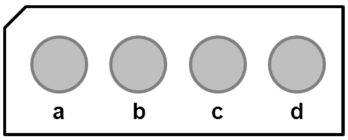

Figure 8 Schematic representation of a membrane in a dot blot hybridization assay. The letters under the dots represent the following yeasts: a: *C. neoformans*, b: MSD44, c: CRUB1564, d: *S. cerevisiae*.

Table 9 Approximate genome size and DNA quantity applied in each dot in dot blot hybridization assays.

	Approximate genome size (Mb)	DNA in dot (ng)
C. neoformans	18.5	200
MSD44[†]	18.5	200
CRUB1564[†]	18.5	200
S. cerevisiae	12.1	135

[†] Genome size of both *Cryptococcus* sp. strains was assumed to be approximately the same as the genome of the type species *C. neoformans*.

The protocol for dot blot hybridization was adapted and optimized from the DIG Application Manual for Filter Hybridization from Roche Molecular Biochemicals: genomic DNA and DIG-labeled probes were denatured by boiling for 10 and 5 min, respectively, and immediately placed on ice. For each dot the corresponding genomic DNA sample volume (5 µL) was placed on the membrane. The DNA samples were allowed to dry and were then fixed to the membrane by baking at 180ºC for 2 hr.

The membranes pre-hybridized with pre-warmed Pre-Hybridization Solution (10 mL; composition of dot blot hybridization solutions is described in Annex IV) for 1 hr at the hybridization temperature (T_{hyb} = 60ºC; optimized empirically) in 50 mL falcon tubes, in a hybridization oven. The Pre-Hybridization Solution was recovered (3.5 mL) and 7 µL of DIG-labeled probe were added (Hybridization Solution). The membranes were allowed to hybridize overnight (approximately 16 hr) at T_{hyb}. Excess and nonspecifically bound DIG-labeled probe was washed with Low (2x 5 min at RT) and High Stringency Buffer (2x 15 min at T_{hyb}), respectively. The membranes were then washed with Washing Buffer and equilibrated in Blocking Solution (40 min at RT). Anti-DIG-AP Antibody (1:5000) was added to 5 mL of recovered Blocking Solution and the membranes were incubated for 30 min. Excess Antibody was removed with Washing Buffer (2x 15 min). The membranes were then equilibrated with Detection Buffer for 3 min and transferred to flat containers. Nitro-blue tetrazolium/5-bromo-4-chloro-3-indolyphosphate p-toluidine salt (NBT/BCIP) Chromogenic Substrate (150 µL) was added to 7.5 mL of Detection Buffer and the membranes were incubated overnight, protected from light. Finally, to stop the revelation step, the Detection Solution was replaced by TE Buffer.

The membranes were then photographed using the UVItec Image System (Cambridge, United Kingdom) with the Alliance Software (Blackburn, Australia). Contrast and brightness were adjusted for better visualization of the dots, using the same software. Finally, the membranes were analyzed by visual assessment of the presence of a positive result (visible dot) or negative result (dot not visible).

Results and discussion

The results of the dot blot hybridization assays are displayed in Figure 9.

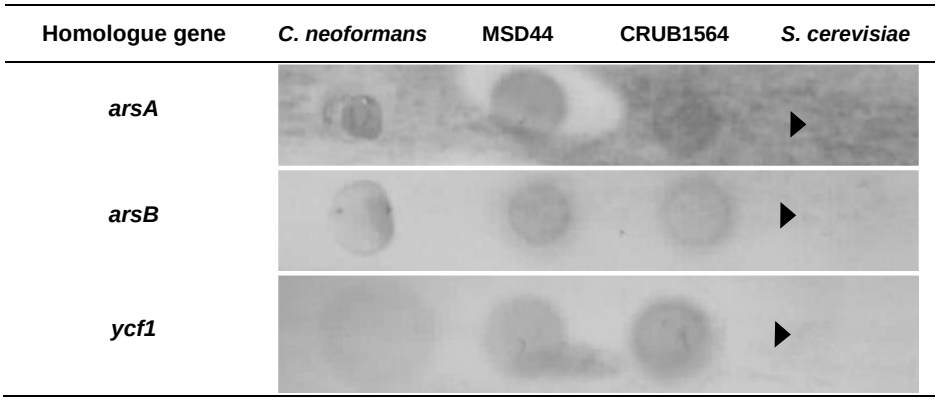

Figure 9 Dot blot hybridization results for the tested probes. Images were obtained with the UVItec Image System (Cambridge, United Kingdom) with the Alliance Software (Blackburn, Australia) and enhanced for contrast and brightness using the same software. Arrows were placed at the left of all applied dots from *S. cerevisiae* to facilitate interpretation.

Homology search in the genomic DNA of MSD44 and CRUB1564 showed positive results for all screened genes at the tested T_{hyb} (Figure 9). These results point to the presence of homologues of the three metal(loid) detoxification associated genes in the genomic DNA of both acidophilic strains.

The results obtained point to the possibility of vacuolar accumulation of thiolated peptides upon exposure to As and Cd in MSD44 and CRUB1564, since both strains presented evidence of the presence of a homologue of the vacuolar transporter Ycf1. Additionally, evidence of As(III) efflux by homologues of the ArsAB complex points to the possibility of As(III) efflux as a detoxification pathway for both strains.

An additional approach was conducted to allow further understanding of Cd detoxification pathways. In this additional molecular approach Cd-induced up-regulated genes were assessed in both acidophilic strains.

7.2. Cd-induced response

RNA extraction and sample preparation

The present molecular approach was conducted to assess the Cd-induced response at a transcriptional level.

Prior to the RNA extraction protocol, the laboratory material used for the RNA extraction and downstream protocols were treated for RNA handling. Metallic spatulas (thoroughly washed) and glass beads (acid-washed, with 425-600 µm, from Sigma-Aldrich, Missouri, USA) were baked at 180ºC overnight (approximately 16h). Supw was treated with 0.01% diethyl pyrocarbonate (DEPC) overnight at 37ºC and autoclaved (15 min at 121ºC). Solutions for RNA extraction and downstream applications were prepared with DEPC-treated supw and new stock reagent solutions. Eppendorf tubes were treated with 0.01% DEPC water overnight at 37ºC and autoclaved.

The protocol used for total RNA extraction was adapted and optimized from the Invitrogen manual for TRIzol reagent: cells grown with and without Cd in scale up conditions (Table 6) were harvested in exponential phase and ressuspended in TRIzol reagent (1 mL per 4-5x10^7 cells) in 1.5 mL eppendorf tubes. After adding approximately 200 µL of treated glass beads, cells were mechanically lysed by vortexing at maximum speed for 2x 2 min. Chloroform purification in the presence of the TRIzol reagent allowed protein and DNA removal. The aqueous phase, containing the total RNA, was transferred to a new eppendorf tube and RNA was precipitated with isopropanol (10 min, at RT). After centrifugation, the resulting pellet was washed with 75% ethanol and allowed to dry before ressuspending in 20 µL DEPC-treated supw. The samples were incubated at 55ºC for 10 min to allow pellet solubilization and stored at -70ºC. RNA quality was determined by gel electrophoresis of total RNA extracts (5 µL from each sample). Total RNA concentration was assessed using a fluorescence-based method with the Qubit RNA Assay Kit, as recommended by the manufacturer, with Qubit fluorometer (Invitrogen, California, USA).

Messenger RNA was purified from total RNA samples with GenElute mRNA Miniprep Kit (Sigma-Aldrich, Missouri, USA), as recommended by the manufacturer. Succinctly, the oligo-d(T) polystyrene beads added to the samples in the spin columns bind to polyadenylated mRNA and, after washing contaminants, the mRNA is recovered in the provided elution solution. After this purification step, the mRNA samples are stored at -70ºC. Messenger RNA concentration was also assessed, in the same manner as described above for total RNA samples.

Suppression subtractive hybridization

The four mRNA samples obtained were subjected to suppression subtractive hybridization (SSH) to allow assessment of differentially expressed transcripts in the presence of Cd. Succinctly, this approach allows selective amplification of differentially expressed and normalized double stranded (ds) cDNA fragments. The subtraction step in SSH ensures that ds cDNAs that correspond to differential transcripts are preferentially present in the final product, as the products commonly expressed in the control (*driver* mRNA) and Cd (*tester* mRNA) growth conditions are subtracted. Additionally, the normalization step in this methodology ensures that low abundance transcripts have a higher probability of being represented in the final product.

SSH was performed with the PCR-Select cDNA Subtraction kit from Clontech (California, USA; Diatchenko *et al.*, 1996) and the experimental protocol was conducted as recommended by the manufacturer: first, mRNA samples (105 ng for MSD44, 85 ng for CRUB1564) were converted into cDNA with AMV Reverse Transcriptase. The second-strand synthesis was performed with an enzyme cocktail containing DNA polymerase I, RNase H and *E. coli* DNA ligase, yielding ds cDNA. Then, the nucleic acid was purified with phenol-chloroform-isoamyl alcohol (25:24:1) and NH_4OAc/ethanol precipitation. Next, tester and driver ds cDNA samples were digested with *Rsa*I, a four-base cutting restriction enzyme that generates shorter, blunt-ended ds cDNA fragments. The resulting ends are optimal for adaptor ligation prior to hybridization. The samples were purified again, as described above.

The resulting ds cDNA samples from driver mRNA were now ready for the hybridization steps. However, the tester ds cDNA fragments had to be ligated to two adaptors (1 and 2R) before the hybridization step took place. Each tester sample was ligated to the adaptors with T4 DNA ligase (overnight at 16ºC). The resulting adaptor-ligated ds cDNA tester fragments were ready for the hybridization steps. Two sequential hybridization steps were performed. In the first, an excess of adaptor-free *Rsa*I-digested driver ds cDNA was added to each corresponding adaptor-ligated *Rsa*I-digested tester ds cDNA. This hybridization occurred by denaturing briefly at 98ºC and annealing for 8 hr at 68ºC. For the second hybridization, fresh denatured adaptor-free *Rsa*I-digested driver ds cDNA and both tester samples were mixed together. This step took place overnight at 68ºC. These hybridization steps allowed normalization and enrichment of differentially expressed transcripts.

The resulting subtracted samples were then subjected to two consecutive PCR amplifications to obtain differentially expressed cDNAs in elevated amounts. For the first PCR reaction (settings in Table 10), only one primer was used. This ‘PCR Primer 1’, provided in the kit, was complementary to the sequence of the adaptors, enabling the exponential amplification of differentially expressed transcripts. Prior to the amplification cycles, the adaptors were extended for 5 min at 72ºC. At this point, non-differentially expressed hybrid sequences were either not amplified or did not have an exponential amplification. Then, a nested PCR was performed, with the adaptor-specific primers 1 and 2R, and the PCR cycling started immediately: 35 cycles as described in Table 10, except with an annealing temperature of 65ºC. The resulting PCR products were enriched for differentially expressed ds cDNAs corresponding to Cd-induced up-regulated transcripts.

The PCR products were purified using the Jetquick PCR Product Purification Spin Kit (Genomed GmbH, Germany) and ligated into the T/A pCR II vector from Invitrogen, using TA Cloning Kit (Invitrogen, California, USA) as recommended by the manufacturer. Consequently, two pools of recombinant vectors were obtained, one for each acidophilic strain.

Table 10 PCR amplification settings for the first PCR reaction in SSH procedure.

Temperature (ºC)	Time (min)	Number of cycles
94	3	1
94	1	34
64	1	
72	1.5	
72	3	1

These recombinant vectors were used to transform chemically competent *E. coli* XL-1 Blue-MRF' cells by applying the heat shock method. 300 µL aliquots of the ampicillin resistant transformed cells were used as inoculum in supplemented Luria Bertani Agar plates (medium composition and preparation in Annex V) to select the transformant clones. Cell lysates from both subtracted lybraries were prepared in 50 µL of TE with 0.1% of Tween 20, by boiling at 100ºC for 10 min. Then, PCR amplification using polylinker-specific primers (settings in Table 11) allowed a screening of the selected 150 clones with assessment of insert size.

Table 11 PCR settings for insert amplification of 150 clones from the subtracted lybraries of MSD44 and CRUB1564.

Temperature (ºC)	Time (min)	Number of cycles
94	3	1
94	1	34
50	1.5	
72	1	
72	3	1

40 of 150 screened clones were selected for sequencing using insert size as criteria to select different products. PCR products were purified with Jetquick PCR Product Purification Spin Kit (Genomed GmbH, Germany) and sequencing was conducted using laboratory sequencing services. The resulting sequences were submitted to a visual correction with Chromas Lite 2.01 software (Technelysium Pty, Australia), and used as a nucleotide query in a search in a non-redundant protein database, using a translated nucleotide query (blastx) in NCBI, using the default settings. The results of this homology search were analyzed considering cutoff values of 70.0 and 10E-10 for score and expected E-value, respectively, as these allowed removal of unspecific homology detection in the blastx search, while maintaining results that clearly reflected homology.

Results and discussion

The results obtained for the homology search (blastx) of the sequenced products are summarized in Table 12 and further details are provided in Table 13.

Table 12 General results of homology search of the subtracted cDNA library obtained from SSH for MSD44 and CRUB1564.

	MSD44	CRUB1564
Number of sequenced products	21	19
Average read length (bp)	312	335
Match with known products	5/21	8/19
Match with products with putative function	2/21	4/19
No match[†]	14/21	7/19

[†]Includes sequences below cutoff values for score (>70.0) and above cutoff for expected E-value (<10E-10). Lack of match in blastx is also considered in these sequences.

Table 13 Putative identification of proteins corresponding to sequences obtained in SSH for both acidophilic strains according to blastx results in NCBI. All results presented below showed homology with sequences from *Cryptococcus neoformans* and *Cryptococcus gattii*. Accession numbers refer to the results for the type species, *C. neoformans*.

	Accession numbers	Frequency	Score	Query length (bp)	Coverage (%)	Max id (%)	E-value
MSD44							
Functional category							
Protein synthesis							
40S ribosomal protein S7	XP_572711.1	2/21	176.0	399	78	87	1E-54
Protein folding							
Cyclophilin A	XP_568796.1	1/21	162.0	372	70	87	1E-49
Hypothetical proteins							
JmjC domain	XP_778339.1	1/21	70.1	123	97	67	1E-14
NADB_Rossmann domain	XP_567473.1	1/21	94.7	419	87	50	5E-22
CRUB1564							
Functional category							
Protein synthesis							
60S ribosomal protein L17	XP_568654.1	1/19	76.3	405	48	63	2E-21
Translation elongation factor 1-α	AAB88586.1	1/19	89.4	246	76	70	6E-20
Translation elongation factor 2	XP_570549.1	5/19	214.0	379	87	92	8E-64
Protein folding							
Cyclophilin A	XP_568796.1	1/19	162.0	337	79	86	6E-50
Hypothetical proteins							
RNA recognition motif	XP_568231.1	4/19	148.0	479	74	66	4E-40

[†]When more than one query showed homology with the same predicted protein, only the queries with higher Score and lower E-value are presented.

Results obtained for homology search with the SSH final products matched sequences from the type species *C. neoformans* and from the related *C. gattii*. Since score and E-value parameters indicated a higher homology to sequences from *C. neoformans* (data not shown), only the accession numbers for the type species are displayed in Table 13.

The results obtained with the SSH methodology and homology search suggest that exposure to Cd leads to the up-regulation of different gene products involved in protein synthesis in both strains, as reflected by the up-regulation of ribosomal proteins and translation elongation factors (Table 13). These results are in agreement with comparative transcriptomic and proteomic studies conducted in *S. cerevisiae*, which showed that several genes involved in protein synthesis are up-regulated upon exposure to Cd (Momose & Iwahashi, 2001; Jin *et al.*, 2008). Other studies report that this enhanced protein synthesis is highly related to sulfur sparing (see Introduction, Figure 2; Fauchon *et al.*, 2002), as enzymes involved in the sulfur amino acid biosynthesis pathway are up-regulated in the presence of Cd and mainly directed to the synthesis of GSH (Fauchon *et al.*, 2002; Vido *et al.*, 2001).

Cyclophilin A is involved in protein folding mechanisms and was detected in both acidophilic strains (Table 13). Enhanced protein folding and stabilization appears to be a general response mechanism in yeasts upon exposure to Cd, as reported by some transcriptomic approaches (Momose & Iwahashi, 2001; Jin *et al.*, 2008). Additionally, the comparative proteomic study from Vido *et al.* (2001) showed that heat shock proteins are highly associated with Cd-response, since many proteins are damaged in the presence of this nonessential metal.

Results from homology search of sequences obtained for the Portuguese strain indicated that proteins containing JmjC domains are up-regulated in response to Cd (Table 13). These domains have Zn-fingers and are part of the cupin superfamily of metalloenzymes (Mosammaparast & Shi, 2010). The JmjC domain has been associated with proteins that directly remove histone lysine methylation via a hydroxylation reaction (Trewick *et al.*, 2005; Kwon & Ahn, 2011), thus participating in histone modifications and regulation of the integrity of the chromatin structure (Clissold & Ponting, 2001). Chromatin modification has been associated with yeasts response to Cd, as several chromatin remodeling complexes were found to be up-regulated upon exposure to this metal (Momose & Iwahashi, 2001; Jin *et al.*, 2008; Ruotolo *et al.*, 2008). These chromatin modification complexes were reported as being able to influence the expression of genes necessary for recovery after exposure to the nonessential metal and. Moreover, these complexes influence DNA reactivity and accessibility to DNA repair enzymes (Ruotolo *et al.,* 2008), which are a target of Cd toxicity (Table 1).

An additional Cd-induced response was observed for MSD44, which is associated with NADB-Rossman domains (Table 13). According to the protein annotation resource Conserved Domains Database (CDD), this domain is found in numerous dehydrogenases of metabolic pathways such as glycolysis, and many other redox enzymes, which typically contain a second domain which is responsible for specifically binding a substrate and catalyzing a particular enzymatic reaction. Proteins that fit this profile, such as enzymes involved in carbohydrate metabolism, were found to be up-regulated in the presence of Cd (Fauchon *et al.*, 2002; Jin *et al.*, 2008). Jin *et al.* (2008) assessed the transcriptomic response to different heavy metals and observed the occurrence of a *common metal response.* The latter corresponds to a general and non-specific response activated upon exposure to different metals and includes enzymes involved in carbohydrate metabolism. Accordingly, in this study, the up-regulation of these proteins in response to Cd may be part of a common response, instead of a Cd-specific mechanism.

In addition to enhanced protein synthesis and folding processes, the obtained results for the Argentinean strain indicate that gene products harboring domains with RNA recognition motifs (RRM) were up-regulated (Table 13). According to CDD, proteins harboring RRM domains are involved in post-transcriptional gene expression processes including mRNA and rRNA processing, RNA export and RNA stability. Nucleocytoplasmic transport was recently implicated in yeast cell recovery and survival mechanisms in response to Cd toxicity by Ruotolo *et al.* (2008). These authors observed that mRNA trafficking is up-regulated upon Cd exposure and suggest that mRNA turnover and relocalization are important factors for translational and metabolic reprogramming under metal stress conditions.

Both in ours and in the abovementioned studies, a considerable percentage of unknown products were up-regulated upon Cd exposure. This reflects how much is still unknown in heavy metal response and detoxification in yeasts and reinforces the necessity to conduct more studies on the subject. In our study in particular, the high number of unmatched products (Table 12) reflects how much is unknown in metal response mechanisms in basidiomycetous yeasts, as the most studied microbes within the group are the clinically relevant *C. neoformans* and *C. gattii*. More importantly, the uniqueness of the species at study suggests that the extreme conditions to which it is constantly exposed probably conditioned the mechanisms used to thrive in such an environment, in a parallel to what has been observed in prokaryotes (Dopson *et al*., 2003; see Introduction). Accordingly, at least part of the unmatched sequences obtained in this approach may correspond to products related to undescribed heavy metal response and resistance mechanisms.

8. Global discussion

In the present work, different approaches were conducted to understand metal(loid) detoxification mechanisms in two acidophilic yeasts from a new *Cryptococcus* species. Considering the results obtained and the information available for metal(loid) detoxification mechanisms in yeasts (described in the Introduction section), a number of hypotheses for mechanisms operating in these strains are proposed below.

8.1. Arsenic resistance

Information available on As detoxification mechanisms describe mainly As(III) detoxification. In fact, the only As(V) detoxification mechanism described in yeasts resides in the reduction of As(V) to As(III) by an As(V) reductase (Mukhopadhyay *et al.*, 2000). Thiol-mediated As(III) detoxification mechanisms include As(III) chelation by thiolated peptides, namely GSH and PC. Subsequently, $As(GS)_3$ complexes may be transported to the vacuole by Ycf1 (Prévéral *et al.*, 2006; reviewed in Tamás & Wysocki, 2010). As(III) detoxification can also be accomplished by metalloid efflux to the outside of the cell, through a number of transporters, not involving thiolated peptides (reviewed in Tamás & Wysocki, 2010). Despite the absence of information in published literature about *C. neoformans*, evidence of homologues of genes related with As(III) detoxification were found in its genome (information based on NCBI database). These include the Ycf1 vacuolar transporter, the As(III) efflux pump ArsB and its associated ATPase ArsA, and the As(III) permease Arr3.

Results obtained for MSD44 and CRUB1564 showed that As resistance levels are not influenced by sulfate availability, and confirmed the higher toxicity of the trivalent chemical form of the metalloid (Table 4 and Figure 5A; Oremland & Stolz, 2003). Additionally, both strains present homology with genes related to As(III) detoxification: *ycf1*, *arsB* and the associated ATPase *arsA* (Figure 9). Intra-specific variability was observed in the cytological approach, as the Portuguese strain presented higher thiol accumulation levels upon exposure to As, while thiol levels did not change for CRUB1564 (Figure 7).

According to the obtained results and the available literature, an As detoxification mechanism common to both acidophilic strains could be attributed to a reduction step of As(V) to As(III) with an As(V) reductase (reviewed in Tamás & Wysocki, 2010). Since both MSD44 and CRUB1564 present homologues of *arsA*, *arsB* and *ycf1* genes, As(III) detoxification may be accomplished by metalloid efflux and vacuolar accumulation simultaneously, as is the case for *S. cerevisiae* with the Arr3 permease and Ycf1 (see Introduction). Considering that accumulation of thiolated peptides upon exposure to As was only observed for the Portuguese strain, a predominant As(III) detoxification mechanism involving the vacuolar sequestration of $As(GS)_3$ conjugates can be suggested for MSD44.

Regarding the involvement of thiolated peptides in response to As toxicity, a phenomenon equivalent to sulfur sparing was observed in response to As exposure in *S. cerevisiae* (Haugen *et al.*, 2004). These authors showed that exposure to As in the baker's yeast lead to an alteration in sulfur and GSH metabolism, resulting in an increased production of GSH. The results observed for the Portuguese strain are in agreement with this possibility of alteration in the sulfur and GSH metabolism directed towards an oxidative stress response, as the thiol content in MSD44 was increased upon exposure to the metalloid.

On the other hand, As-induced intracellular thiol accumulation was not observed for CRUB1564, suggesting that this strain predominantly resists As by detoxification mechanisms that do not involve accumulation of thiolated peptides, such as As(III) extrusion by the abovementioned ArsAB pump.

It should be noted that low sensitivity to small variations of fluorescence intensity may represent a limitation inherent to the applied cytological methodology. Accordingly, although the results for CRUB1564 do not point to an enhanced thiol accumulation induced by As, the possibility of GSH production to cope with oxidative stress cannot be excluded, seen as this thiolated peptide is the central antioxidant in yeast cells (Zechmann *et al.*, 2011).

Protein activity studies should be conducted in future investigation to confirm As(III) efflux activity by ArsAB homologues and vacuolar accumulation by a Ycf1-like transporter in both acidophilic strains.

8.2. Cadmium resistance

Cd detoxification mechanisms described in yeasts highly suggests Cd chelation by the thiolated peptides GSH and PCs, resulting in Cd-thiolated peptide complexes (reviewed in Tamás & Wysocki, 2010), with subsequent vacuolar accumulation through Ycf1 (Li *et al.*, 1997) or Hmt1 (Prévéral *et al.*, 2006 and 2009), respectively. Additionally, $Cd(GS)_2$ complexes were shown to be the substrate of the Cd efflux pump Yor1 (Nagy *et al.*, 2006). Moreover, Cd-induced sulfur sparing was described as shifting the intracellular sulfur pool to GSH production to cope with Cd toxicity (Figure 2; Fauchon *et al.*, 2002). In fact, only one detoxification mechanism was described in yeasts as not involving thiolated peptides: the Cd efflux pump Pca1 (Figure 1B; Adle *et al.*, 2007).

The results obtained for the Argentinean strain highly point to an involvement of thiolated peptides in the Cd response: (i) MIC determination results showed that the lowest Cd resistance level was associated with the condition with less available sulfate (Table 4 and Figure 5B); (ii) a clear thiol accumulation was observed upon Cd exposure in the cytological approach (Figure 7; RFI=1.83); (iii) evidence of a homologue of a $Cd(GS)_2$ vacuolar transporter was found (Figure 9). On the other hand,

the only evidence found linking Cd detoxification to thiolated peptides in MSD44 is related with the positive result for search of a *ycf1* gene homologue (Figure 9). Nevertheless, this positive result can be related only to As(III) detoxification (as discussed above) and not to Cd detoxification, since Ycf1 uses $As(GS)_3$ and $Cd(GS)_2$ conjugates as a substrate for transport (reviewed in Tamás & Wysocki, 2010).

A common Cd response could be present in both acidophilic strains, based on *de novo* protein synthesis and folding, which were found to be involved in the response to this heavy metal by the conducted transcriptomic approach. Also, since the Cd resistance levels are very high in MSD44 and CRUB1564, an efflux mechanism can be involved in Cd resistance in both strains, possibly through a homologue of the transporter Pca1, since this transporter is described as being capable of an efficient Cd detoxification (Adle *et al.*, 2007).

Considering the abovementioned results and background information, Cd detoxification in MSD44 would mainly operate via a Pca1-like efflux pump, since it is the only mechanism described that does not involve thiolated peptides.

On the other hand, since thiols are clearly involved in Cd detoxification for the Argentinean strain and evidence of increased protein synthesis was observed in the SSH approach (Table 13), a possible sulfur sparing setting can be involved in the Cd response in this strain. This hypothesis would result in an elevated intracellular GSH content which could chelate the nonessential metal, forming $Cd(GS)_2$ complexes and possibly lead to subsequent vacuolar accumulation through a homologue of Ycf1 (reviewed in Tamás & Wysocki, 2010) or Hmt1 (Prévéral *et al.*, 2009). Alternatively, GSH could be used as a substrate for Cd-induced PC synthesis, resulting in the formation of Cd-PC complexes, with possible subsequent vacuolar accumulation through a homologue of the Hmt1 transporter (Prévéral *et al.*, 2009).

Further investigation is needed in several aspects to fully assess Cd detoxification mechanisms in these acidophilic strains. First, the sulfur sparing possibility proposed for the Argentinean strain should be assessed by analyzing alterations in the sulfur metabolism proteins in the presence of Cd. Furthermore, the possibility of a Pca1-like transporter should be assessed by homology search and subsequent gene expression assays.

8.3. Copper resistance

Two main detoxification mechanisms are described in yeasts for Cu detoxification. The first associates the production of the Cup1 MT in response to Cu excess (reviewed in Tamás & Wysocki, 2010). The second mechanism involves Cu transport to the outside of the cell and was described as conferring relatively elevated resistance levels to the yeast *C. albicans* (Weissman *et al*., 2000).

Results for the Argentinean strain in the physiological approach clearly reflected sulfate dependency upon exposure to Cu (Figure 5C and 6; Table 4 and 5). Results for CMFDA staining in this strain also support the involvement of sulfur in Cu detoxification, since thiol accumulation was observed in response to the presence of Cu. Subsequently, a thiol-mediated mechanism for Cu resistance is in agreement with the obtained results, possibly involving participation of MTs in a Cup1-like setting (Figure 1C; reviewed in Tamás & Wysocki, 2010). Nevertheless, other thiolated peptides, such as GSH and/or PCs may be involved in this response, although not described as being chiefly involved with Cu detoxification in yeasts. To understand if this thiol-mediated Cu detoxification response is being mediated by a MT, a Northern blot experiment could be performed, using conserved sequences as a probe.

The results obtained for the Portuguese strain also point to an influence of sulfate availability and the involvement of thiolated peptides in Cu detoxification: (i) MIC determination results and subsequent statistical analysis showed that this strain resists higher Cu concentrations in the condition with most available sulfate (Figure 5C); (ii) the differential staining in cytological assays pointed to thiol accumulation upon exposure to Cu (Figure 7). However, this strain showed much higher resistance to this heavy metal (Figure 5C). Considering these results, a basal mechanism involving thiolated peptides may be suggested, similar to the one suggested above for the Argentinean strain. Nevertheless, taking into account the higher resistance levels observed for MSD44, an additional Cu detoxification mechanism, not involving thiolated peptides, can be suggested for this strain. Accordingly, further Cu detoxification may be achieved in the Portuguese strain by exporting this metal to the outside of the cell through a Crp1-like transporter, as is the case in *C. albicans* (Weissman *et al.*, 2000).

Assessment of MT-mediated Cu detoxification should be assessed as described above for CRUB1564. Moreover, the presence of a Crp1-like transporter should be evaluated by homology search using conserved regions of this transporter as a probe.

8.4. Zinc resistance

As was denoted before, the main Zn detoxification mechanism identified so far in yeasts consists in vacuolar accumulation of this metal (Figure 1D; Simm *et al.*, 2007). An alternative intracellular accumulation mechanism was identified in the fission yeast *S. pombe* and relies on Zn accumulation in the endoplasmic reticulum (Borrelly *et al.*, 2002). Additionally, a thiol-mediated mechanism was described in different ascomycetous yeasts, where MTs are synthesized in response to exposure to excess Zn (Pagani *et al.*, 2007a; Borrelly *et al.*, 2002).

The results obtained in this study revealed that sulfate availability influences Zn resistance levels in the Portuguese strain in three different aspects: (i) the lower MIC value observed was obtained for the condition with less available sulfate (Figure 5D); (ii) statistical analysis of AUCx in the evaluated *m*MTCs showed that yeast growth is superior in Sulfate-YNB medium (Table 4); (iii) a decrease in thiol accumulation was observed upon Zn exposure (Figure 7A; $ZnSO_4$), which was reflected by an RFI value of 0.77 (Figure 7B; $ZnSO_4$). This Zn-induced thiol pool depletion was observed in yeasts before, by Pagani *et al.* (2007b). These authors reported that the presence of excess Zn induced an oxidative stress response in the yeast cell, followed by a consumption of low-molecular weight thiols, namely GSH. Considering this information, MSD44 may respond to Zn surplus by consuming thiols, possibly GSH as a means to cope with Zn-induced oxidative stress, thus supporting the need for sulfate availability in the growth medium. Moreover, an additional Zn detoxification mechanism mediated by metal accumulation in an intracellular compartment may be suggested, seen as higher than average resistance levels were observed. Such intracellular accumulation could be directed to the vacuole, through a Cot1-like or Zrc1-like transporter, or to the endoplasmic reticulum, through a Zhf1-like transporter.

The results obtained for the Argentinean strain only point to the possibility of sulfate availability influence upon analysis of the determined MIC values, seen as the MIC determined for the condition with most sulfate is double the MICs obtained in all other conditions (Figure 5D). However, statistical analysis of average growth revealed that AUCx was equivalent in all tested conditions. Considering this, the hypothesis of Zn-induced MT synthesis could be evaluated, as it would account for a higher demand for sulfate availability in the growth medium. However, differential thiol accumulation was not observed upon exposure to Zn in this strain (Figure 7). Accordingly, the predominant mechanism of Zn detoxification in CRUB1564 may rely on intracellular accumulation in organelles such as the vacuole or the endoplasmic reticulum, through homologues of the abovementioned transporters.

Considering that the proposed Zn detoxification mechanisms involve different subcellular compartments, further understanding of the detoxification mechanism(s) operating in *Cryptococcus* sp. could be explored using fluorescence microscopy with a Zn-specific probe and adequate organelle-specific probes. This methodology would allow visualization of the subcellular compartment that stores Zn upon exposure to elevated concentrations: vacuole, endoplasmic reticulum, both, or neither – the latter situation suggesting an alternative mechanism.

9. Final considerations

In the present work, heavy metal(loid) detoxification mechanisms were assessed in two strains from geographically distinct backgrounds, belonging to a new and unique acidophilic yeast species.

Overall, the results obtained suggest intra-specific variability in detoxification mechanisms that operate upon metal(loid) exposure. This was particularly observed for Cu resistance, since the Argentinean strain revealed a sulfate dependency upon exposure to toxic concentrations of this heavy metal. Seen as the Portuguese strain is exposed to very high concentrations of Cu in its natural environment (Table 2), it could be hypothesized that the different backgrounds that MSD44 and CRUB1564 are exposed to may have influenced the evolution of metal detoxification mechanisms.

Despite the fact that some results obtained throughout this study are in agreement with mechanisms already described in neutrophilic yeasts, novel heavy metal(loid) detoxification mechanisms may be accountable for the overall higher resistance levels presented by the tested strains of *Cryptococcus* sp.. These high resistance levels may be associated with a higher number of copies of genes related to metal(loid) detoxification, enhanced expression of those genes upon metal(loid) exposure, or undescribed resistance mechanisms.

Further investigation should be pursued for all tested metal(loid)s, to disclose which mechanisms are associated with each metal(loid) and to understand how these microbes thrive in such extreme environments.

10. Bibliographic references

Adle DJ, Sinani D, Kim H & Lee J (2007) A Cadmium-transporting P1B-type ATPase in yeast *Saccharomyces cerevisiae*. J Biol Chem 282:947-955.

Altschul SF, Gish W, Miller W, Myers EW & Lipman DJ (1990) Basic local alignment search tool. J Mol Biol 215:403-410.

Beaudoin J, Thiele DJ, Labbé S & Puig S (2011) Dissection of the relative contribution of the *Schizosaccharomyces pombe* Ctr4 and Ctr5 proteins to the copper transport and cell surface delivery functions. Microbiology 157:1021-1031.

Begot C, Desnier I, Daudin JD, Labadie JC & Lebert A (1996) Recommendations for calculating growth parameters by optical density measurements. J Microbiol Methods 25:225-232.

Beyersmann D & Hartwig A (2008) Carcinogenic metal compounds: recent insight into molecular and cellular mechanisms. Arch Toxicol 82:493-512.

Borrelly GPM, Harrison MD, Robinson AK, Cox SG, Robison NJ & Whitehall SK (2002) Surplus zinc is handled by Zym1 metallothionein and Zhf endoplasmic reticulum transporter in *Schizosaccharomyces pombe*. J Biol Chem 277:30394-30400.

Carri MT, Galiazzo F, Ciriolo MR & Rotilio G (1991) Evidence for co-regulation of Cu, Zn superoxide dismutase and metallothionein gene expression in yeast through transcriptional control by copper via Ace1 factor. FEBS Lett 278:263-266.

Clemens S, Kim EJ, Neumann D & Schroeder JI (1999) Tolerance to toxic metals by a gene family of phytochelatin synthases from plants and yeast. EMBO J 18:3325-3333.

Clissold PM & Ponting CP (2001) JmjC: cupin metalloenzyme-like domains in jumonji, hairless and phospholipase A2beta. Trends Biochem Sci 26:7-9.

Dancis A, Haile D, Yuan DS & Klausner RD (1994) The *Saccharomyces cerevisiae* copper transport protein (Ctr1p). Biochemical characterization, regulation by copper, and physiologic role in copper uptake. J Biol Chem 269:25660-25667.

De Silóniz MI, Payo EM, Callejo MA, Marquina D & Peinado JM (2002) Environmental adaptation factors of two yeasts isolated from the leachate of a uranium mineral heap. FEMS Microbiol Lett 210:233-237.

Diatchenko L, Lau YFC, Campbell AP, Chenchik A, Moqadam F, Huang B, Lukyanov S, Lukyanov K, Gurskaya N, Sverdlov ED & Siebert PD (1996) Suppression subtractive hybridization: a method for generating differentially regulated or tissue-specific cDNA probes and libraries. Biochemistry 93:6025-6030.

Dopson M, Baker-Austin C, Koppineedi PR & Bond PL (2003) Growth in sulfidic mineral environments: metal resistance mechanisms in acidophilic micro-organisms. Microbiology 149:1959-1970.

Duffus JH (2002) "Heavy metals" – a meaningless term. Pure Appl Chem 74:793-807.

Fauchon M, Lagniel G, Aude JC, Lombardia L, Soularue P, Petat C, Marguerie G, Sentenac A, Werner M & Labarre J (2002) Sulfur sparing in the yeast proteome in response to sulfur demand. Mol Cell 9:713-723.

Gadanho M & Sampaio JP (2006) Microeukaryotic diversity in the extreme environments of the Iberian Pyrite Belt: a comparison between universal and fungi-specific primer sets, temperature gradient gel electrophoresis and cloning. FEMS Microbiol Ecol 57:139-148.

Gadanho M, Libkind D & Sampaio JP (2006) Yeast Diversity in the Extreme Acidic Environments of the Iberian Pyrite Belt. Microb Ecol 52:552-563.

Gross S & Robbins EI (2000) Acidophilic and acid-tolerant fungi and yeasts. Hydrobiologia 433:91-109.

Hall JL (2002) Cellular mechanisms for heavy metal detoxification. J Exp Bot 366:1-11.

Haugen AC, Kelley R, Collins JB, Tucker CJ, Deng C, Afshari CA, Brown JM, Ideker T & van Houten B (2004) Integrating phenotypic and expression profiles to map arsenic-response networks. Genome Biol 5:R95.

Jin YH, Dunlap PE, McBride SJ, Al-Refai H, Bushel PR & Freedman JH (2008) Global transcriptome and deletome profiles of yeast exposed to transition metals. PLoS Genet 4:e1000053.

Johnson DB & Hallberg KB (2003) The microbiology of acidic mine waters. Res Microbiol 154:466-473.

Kneer R, Kutchan TM, Hochberger A & Zenk MH (1992) *Saccharomyces cerevisiae* and *Neurospora crassa* contain heavy metal sequestering phytochelatin. Arch Microbiol 157:305-310.

Kwon DW & Ahn SH (2011) Role of yeast JmjC-domain containing histone demethylases in actively transcribed regions. Biochem Biophys Res Commun 410:614-619.

Li ZS, Lu YP, Zhen RG, Szczypka M, Thiele DJ & Rea PA (1997) A new pathway for vacuolar cadmium sequestration in *Saccharomyces cerevisiae*: YCF1-catalyzed transport of bis(glutathionato)cadmium. Biochemistry 94:42-47.

Lide DR, editor (2009) CRC handbook of chemistry and physics, 89th edition. Florida, USA: CRC Press.

López-Archilla AI, Marin I & Amils R (2001) Microbial Community Composition and Ecology of an Acidic Aquatic Environment: The Tinto River, Spain. Microb Ecol 41:20-35.

Maciaszczyk-Dziubinska E, Migdal I, Migocka M, Bocer T & Wysocki R (2010a) The yeast aquaglyceroporin Fps1p is a bidirectional arsenite channel. FEBS Lett 584:726-732.

Maciaszczyk-Dziubinska E, Wawrzycka D, Sloma E, Migocka M & Wysocki R (2010b) The yeast permease Acr3p is a dual arsenite and antimonite plasma membrane transporter. Biochim Biophys Acta 1798:2170-2175.

Momose Y & Iwahashi H (2001) Bioassay of cadmium using a DNA microarray: genome-wide expression patterns of Saccharomyces cerevisiae response to cadmium. Environ Toxicol Chem 20:2353-2360.

Mosammaparast N & Shi Y (2010) Reversal of histone methylation: biochemical and molecular mechanisms of histone demethylases. Annu Rev Biochem 79:155-179.

Mukhopadhyay R, Shi J & Rosen BP (2000) Purification and characterization of ACR2p, the Saccharomyces cerevisiae arsenate reductase. J Biol Chem 275:21149-21157.

Nagy Z, Montigny C, Leverrier P, Yeh S, Goffeau A, Garrigos M & Falson P (2006) Role of the yeast ABC transporter Yor1p in cadmium detoxification. Biochimie 88:1665-1671.

Oremland RS & Stolz JF (2003) The ecology of arsenic. Science 300:939-944.

Pagani MA, Villarreal L, Capdevila M & Atrian S (2007a) The *Saccharomyces cerevisiae* Crs5 Metallothionein metal-binding abilities and its role in the response to zinc overload. Mol Microbiol 63:256-269.

Pagani MA, Casamayor A, Serrano R, Atrian S & Ariño J (2007b) Disruption of iron homeostasis in *Saccharomyces cerevisiae* by high zinc levels: a genome-wide study. Mol Microbiol 65:521-537.

Peña MM, Puig S & Thiele DJ (2000) Characterization of the *Saccharomyces cerevisiae* high affinity copper transporter Ctr3. J Biol Chem 275:33244-33251.

Pedrozo F, Kelly L, Diaz M, Temporetti P, Baffico G, Kringel R, Friese K, Mages M, Geller W & Woelfl S (2001) First results on the water chemistry, algae and trophic status of an Andean acidic lake system of volcanic origin in Patagonia (Lake Caviahue). Hydrobiologia 452:129-137.

Perego P & Howell SB (1997) Molecular mechanisms controlling sensitivity to toxic metal ions in yeast. 147:312-318.

Prévéral S, Ansoborlo E, Mari S, Vavasseur A & Forestier C (2006) Metal(loid)s and radionuclides cytotoxicity in *Saccharomyces cerevisiae*. Role of YCF1, glutathione and effect of buthionine sulfoximine. Biochimie 88:1651-1663.

Prévéral S, Gayet L, Moldes C, Hoffmann J, Mounicou S, Gruet A, Reynaud F, Lobinsky R, Verbavatz JM, Vavasseur A & Forestier C (2009) A common highly-conserved cadmium detoxification mechanism from bacteria to humans. Heavy metal tolerance conferred by the ABC transporter SpHMT1 requires glutathione but not metal-chelating phytochelatins peptides. J Biol Chem 284:4936-4943.

Raspor P & Zupan J (2006) Yeasts in extreme environments. Yeast Handbook, Biodiversity and Ecophysiology of Yeasts (Rosa CA & Péter G eds) pp.371-417. Springer-Verlag, Berlin.

Rosen BP (2002) Biochemistry of arsenic detoxification. FEBS Lett 529:86-92.

Ruotolo R, Marchini G & Ottonello S (2008) Membrane transporters and protein traffic networks differentially affecting metal tolerance: a genomic phenotyping study in yeast. Genome Biol 9:R67.

Russo G, Libkind D, Sampaio JP & van Broock MR (2008) Yeast diversity in the acidic Rio Agrio-Lake Caviahue volcanic environment (Patagonia, Argentina). FEMS Microbiol Ecol 65:415-424.

Samikkannu T, Chen CH, Yih LH, Wang AS, Lin SY, Chen TC & Jan KY (2003) Reactive oxygen species are involved in arsenic trioxide inhibition of pyruvate dehydrogenase activity. Chem Res Toxicol 16:409-414.

Sharma KG, Mason DL, Liu G, Rea PA, Bachhawat AK & Michaelis S (2002) Localization, regulation, and substrate transport properties of Bpt1p, a *Saccharomyces cerevisiae* MRP-type ABC transporter. Eukaryot Cell 1:391-400.

Simm C, Lahner B, Salt D, LeFurgey A, Ingram P, Yandell B & Eide DJ (2007) Saccharomyces cerevisiae vacuole in zinc storage and intracellular zinc distribution. Eukaryot Cell 6:1166-1177.

Summers AO (2009) Damage control: regulating defenses against toxic metals and metalloids. Curr Opin Microbiol 12:138–144.

Suzuki T, Yokoyama A, Tsuji T, Ikeshima E, Nakashima K, Ikushima S, Kobayashi C & Yoshida S (2011) Identification and characterization of genes involved in glutathione production in yeast. J Biosci Bioeng 112:107-113.

Tamás MJ & Wysocki R (2001) Mechanisms involved in metalloid transport and tolerance acquisition. Curr Genet 40:2-12.

Tamás MJ, Labarre J, Toledano M & Wysocki R (2006) Molecular Biology of Metal Homeostasis and Detoxification. Top Curr Genet 14:395-454.

Tamás MJ & Wysocki R (2010) How *Saccharomyces cerevisiae* copes with toxic metals and metalloids. FEMS Microbiol Rev 34:925-951.

Thorsen M, Perrone GG, Kristiansson E, Traini M, Ye T, Dawes IW, Nerman O & Tamás MJ (2009) Genetic basis of arsenite and cadmium tolerance in *Saccharomyces cerevisiae*. BMC Genomics 10:105.

Trewick SC, McLaughlin PJ & Allshire RC (2005) Methylation: lost in hydroxylation? EMBO Rep 6:315-320.

Tsai SL, Singh S & Chen W (2009) Arsenic metabolism by microbes in nature and the impact on arsenic remediation. Curr Opin Biotechnol 20:659-667.

Vido K, Spector D, Lagniel G, Lopez S, Toledano MB & Labarre J (2001) A proteome analysis of the cadmium response in *Saccharomyces cerevisiae*. J Biol Chem 276:8469-8474.

Waldron KJ, Rutherford JC, Ford D & Robinson NJ (2009) Metalloproteins and metal sensing. Nature 460:823-830.

Weissman Z, Berdicevsky I, Cavari BZ & Kornitzer D (2000) The high copper tolerance of *Candida albicans* is mediated by a P-type ATPase. Proc Natl Acad Sci 97:3520-3525.

Yuan DS, Dancis A & Klausner RD (1997) Restriction of copper export in *Saccharomyces cerevisiae* to a late Golgi or post-Golgi compartment in the secretory pathway. J Biol Chem 272:25787-25793.

Zar JH (1999) Biostatistical analysis, 4th edition. New Jersey, USA: Prentice Hall, Upper Saddle River.

Zechmann B, Liou LC, Koffler BE, Horvat L, Tomašić A, Fulgosi H & Zhang Z (2011) Subcellular distribution of glutathione and its dynamic changes under oxidative stress in the yeast *Saccharomyces cerevisiae*. FEMS Yeast Res 11:631:642.

Zettler LAA, Gómez F, Zettler E, Keenan BG, Amils R & Sogin ML (2002) Eukaryotic diversity in Spain's River of Fire. Nature 417:137.

11. Annexes

Annex I – Solid MYP preparation

Solid MYP medium was prepared as stated in Table 12 and sterilized by autoclave (15 min at 121ºC). The pH was then adjusted to 3.0 with H_2SO_4 for the acidophilic strains.

Table 14 Final concentration (% w/v) for components of solid MYP medium (adapted from Gadanho *et al.*, 2006).

% w/v	Component
0.7	Malt extract
0.25	Yeast extract
1.7	Peptone
1.7	Agar

Annex II – Liquid YNB preparation

Liquid yeast nitrogen base (YNB) was prepared as stated in Table 13. The pH of the growth medium was adjusted to 3.0 with H_2SO_4. After pH adjustment, the growth medium was sterilized by filtration with syringe filters (pore diameter of 0.22 µm) and stored in falcon tubes at RT.

Table 15 Final concentration (% w/v) for components of liquid YNB medium, according to the manufacturer's instructions (Sigma-Aldrich, Missouri, USA).

% w/v	Component	
0.001	L-histidine	
0.002	DL-methionine	
0.002	DL-tryptophan	
0.5	Glucose	
0.17	Yeast Nitrogen Base	
0.66	$(NH_4)_2SO_4$	Sulfate-YNB
0.53	NH_4Cl	Chloride-YNB

Annex III – DNA extraction solutions

Lysis Buffer: 50 mM Tris, 250 mM NaCl, 50 mM EDTA, 0.3% SDS, pH adjusted to 8.0.

TE Buffer: 10 mM Tris, 1 mM EDTA, pH 8.0. Also used in Dot blot hybridization.

Annex IV – Dot blot hybridization solutions

Pre-hybridization Solution: 5X SSC, 0.1% Sarcosil, 0.02% SDS and 1X Blocking Reagent[†].

Low Stringency Buffer: 2X SSC and 0.1% SDS.

High Stringency Buffer: 0.5X SSC and 0.1% SDS.

Maleic Acid Buffer: 0.1 M Maleic acid, 0.15 M NaCl; adjusted to pH 7.5 with solid NaOH.

Washing Buffer: 0.1 M Maleic Acid Buffer, 0.3% (v/v) Tween 20, 0.15 M NaCl.

Blocking Solution: 1X Blocking Reagent[†] in 0.1 M Maleic Acid Buffer.

Detection Buffer: 0.1 M Tris-HCl, 0.1 M NaCl, pH 9.5.

Detection Solution: 1:50 NBT/NCIP Chromogenic Substrate[†] diluted in Detection Buffer.

TE Buffer: see Annex III.

[†]Blocking Reagent and NBT/NCIP Chromogenic Substrates were provided in the DIG High Prime DNA Labeling and Detection Starter Kit I from Roche Applied Science (Mannheim, Germany).

Annex V – Luria Bertani solid medium preparation

Luria Bertani Agar (LBA) medium was prepared as stated in Table 14 and sterilized by autoclave (15 min at 121ºC).

Table 16 Final concentration (% w/v) for components of solid LBA medium.

% w/v	Component
1	Tryptone
0.5	Yeast extract
0.5	NaCl
1.5	Agar

The following supplements were added to sterile liquefied LBA:

- Ampicillin, 100 µg mL^{-1}
- Isopropyl-β-D-thiogalactoside (IPTG), 80 µg mL^{-1}
- 5-bromo-4-chloro-3-indolyl-beta-D-galactopyranoside (X-Gal), 80 µg mL^{-1}